AN ABSTRACT OF THE THESIS OF

Tullia Leona Upton for the degree of Master of Science in Environmental Science presented on December 6, 2017

Title: Environmental Magnetism as a Proxy for Heavy Metal Concentrations at Formosa Mine Superfund Site

Abstract approved: _____

Joseph S. Stoner

Environmental magnetic techniques have been used to discriminate sources of sediments from a variety of natural and anthropogenic sources. In many studies, magnetic properties such as susceptibility, have served as a proxy for heavy metal concentrations. In these cases, there tends to be enhancement of magnetic minerals. The study presented here explores the application of environmental magnetic measurements as a proxy for heavy metal concentrations from the Formosa Mine Superfund site. It was hypothesized that a similar pattern would be seen when comparing sediments from the mine to sediments downstream from the site and also that magnetic susceptibility and/or isothermal remanent magnetization might provide a useful tool for assessing relative concentrations of heavy metals. The results suggest that there are no significant correlations between heavy metals concentrations and magnetic properties and that processes at the mine have led to depletion of magnetic minerals from the sediments at the mine relative to those downstream.

Environmental Magnetism as a Proxy for Heavy Metal Concentrations at Formosa Mine Superfund Site

by
Tullia Leona Upton

A THESIS

submitted to

Oregon State University

in partial fulfillment of
the requirements for the
degree of

Master of Science

Presented December 6, 2017
Commencement June 2018

Master of Science thesis of Tullia Leona Upton presented on December 6, 2017

APPROVED:

Major Professor, representing Environmental Sciences

Director of the Environmental Science Graduate Program

Dean of the Graduate School

I understand that my thesis will become part of the permanent collection of Oregon State University libraries. My signature below authorizes release of my thesis to any reader upon request.

Tullia Leona Upton, Author

ACKNOWLEDGEMENTS

The author expresses sincere appreciation for the support and assistance of her committee members; Dr. Joseph Stoner, Dr. Carolyn Fonyo, Dr. Mohammad Azzizian, Dr. Julia Jones and Dr. Roberta Hall. She would also like to thank her mother, Kathie Upton for her endless encouragement and support and her fiancé Ryan C'deBaca for his patience and understanding.

In addition, the author would like to acknowledge the administrative staff and faculty at Oregon State University as well as the Fulbright Program for giving her many opportunities to bring outreach and education to communities throughout the state of Oregon. Last, but not least, the author would like to thank her four footed friends, Harley and Fred for providing snuggles and unconditional love as well as a reason to get out of bed on those days which seemed impossible to bare.

TABLE OF CONTENTS

Page

LIST OF FIGURES

Page

LIST OF TABLES

Page

Introduction

Abandoned mines represent a threat to humans and wildlife around the world. They are a source of acid rock drainage (ARD) to surface and groundwater generated by discarded mining materials and underground tunneling. Dusts created during excavation transportation are a source of air pollution near mines. Species living in areas where mining occurs are threatened by ARD, toxic sediments and air pollutants from the mines. It is estimated that there are over 500,000 abandoned mines in the United States with approximately 5827 in Oregon alone (BLM, 2015). With increasing populations and demand for outdoor recreation the potential for hazardous exposure increases as people may be unaware of abandoned mines or the hazards of unidentified features such as mine shafts or mining influenced water (MIW).

In the US, many abandoned mines become designated as Superfund sites. As such, they are placed on a National Priorities List (NPL) for clean-up and remediation by the Environmental Protection Agency (EPA). There are over 1000 Superfund sites in the US, including the Formosa Superfund site in Riddle, OR which was placed on the NPL in 2007. This affected area, which is estimated to be over 75 acres, will be treated according to the plans laid out in the final record of decision for the site. Referred to as remedies, plans include excavation of waste rock and affected sediments near the headwaters of South Fork Middle Creek and Middle Creek, construction of a containment facility to prevent leaching of metals into soils and reworking of roads and flow paths to divert water away from the affected streams.

The site is a continual source of debate and disagreement between stakeholders including local residents, timber companies, BLM, Douglas County officials, the Cow Creek Band of Umpqua Tribe of Indians and the EPA. There are several political divides that impede progress with respect to reclamation or remediation. Some groups want to see the mine re-open while others plead for remediation of the site. While the latter option poses many questions about how to effectively stop ARD at this site, the former offers potential opportunity for employment in an area that is economically disadvantaged. Efforts to clean the site have been unsuccessful, and there is no body or entity to hold accountable for the mess.

There are several techniques employed to survey identified sites that include geochemical analyses and field tests to assess the extent and degree of contamination from various sources. As with any monitoring, it is desirable to have quick and inexpensive methods to do reconnaissance and identify target areas for further investigation. Magnetic measurements have emerged as a plausible technique for monitoring pollution from a number of anthropogenic sources including smelting(e.g. Zhang et al., 2011), vehicle emissions (e.g. Hoffmann et al., 1999; Zhang et al., 2012) and wastewater discharges from a number of industrial processes (e.g. Zhang et al., 2013).

The effectiveness of magnetic techniques to discriminate sediments of anthropogenic genesis from native sediments depends on there being a notable contrast of one or more magnetic properties between native sediments and those derived from anthropogenic sources (Thompson and Oldfield, 1986). Generally, these differences are found in susceptibility (X), isothermal remanence (IRM) or anhysteric remanent magnetization (ARM) (Liu et al., 2012; Thompson and Oldfield, 1986; Verosub and Roberts, 1995). These three properties are indictors and various ratios derived from them yield further information about dominant magnetic mineralogy and grain size which may change due to natural or anthropogenic processes (Maher and Thompson, 1999; Oldfield et al., 1985; Thompson and Oldfield, 1986).

It is proposed that environmental magnetic techniques may be used to discriminate the anthropogenically derived sediments from naturally occurring sediments at the Formosa Mine Superfund site near Riddle, OR. If so, there will be specific magnetic properties that are characteristic of background materials compared to mining materials found onsite. Results suggest that materials downstream from the affected area consist of coarser grained materials which maintain higher remanence than the materials from the Formosa Mine and that the silt fraction (20-63μm) carries the magnetic signature that allows for discrimination of background material from materials affected by mining processes.

Hypotheses

Anthropogenically derived sediments from various industrial processes have enhanced magnetic susceptibility and coarse magnetic grain sizes. It is hypothesized that sediments affected by mining activities will have higher magnetic susceptibility and coarser grain sizes compared to sediments taken from downstream. If this is true, sediments from the mine will have higher X and lower SIRM/X values compared to the sediments collected downstream.

It is also hypothesized that sediments from the mine will have higher concentrations of heavy metals (Fe, V, Ti, Ni, Cu, Cd, As and Mn) compared to sediments collected downstream. There are various processes and conditions that lead to mobilization, precipitation and adsorption of metals to iron bearing minerals which occur at the mine which would contribute to higher concentrations of metals at the Formosa Mine.

Background

Study Area

Formosa Mine is located approximately 25 miles south of Roseburg, OR in the Coastal ranges of the Klamath Mountains (see Figure 1). The area is characterized by steep slopes and narrow ridges that delineate several sub-watersheds in the southern parts of the Umpqua Watershed. Landownership is mixed and consists of private land owned by Formosa Exploration Incorporated (the mining company), the Bureau of Land Management (BLM) and Douglas County (CDM, 2009). Adjacent lands are privately owned by timber companies and private landowners as well as the BLM (CDM, 2009).

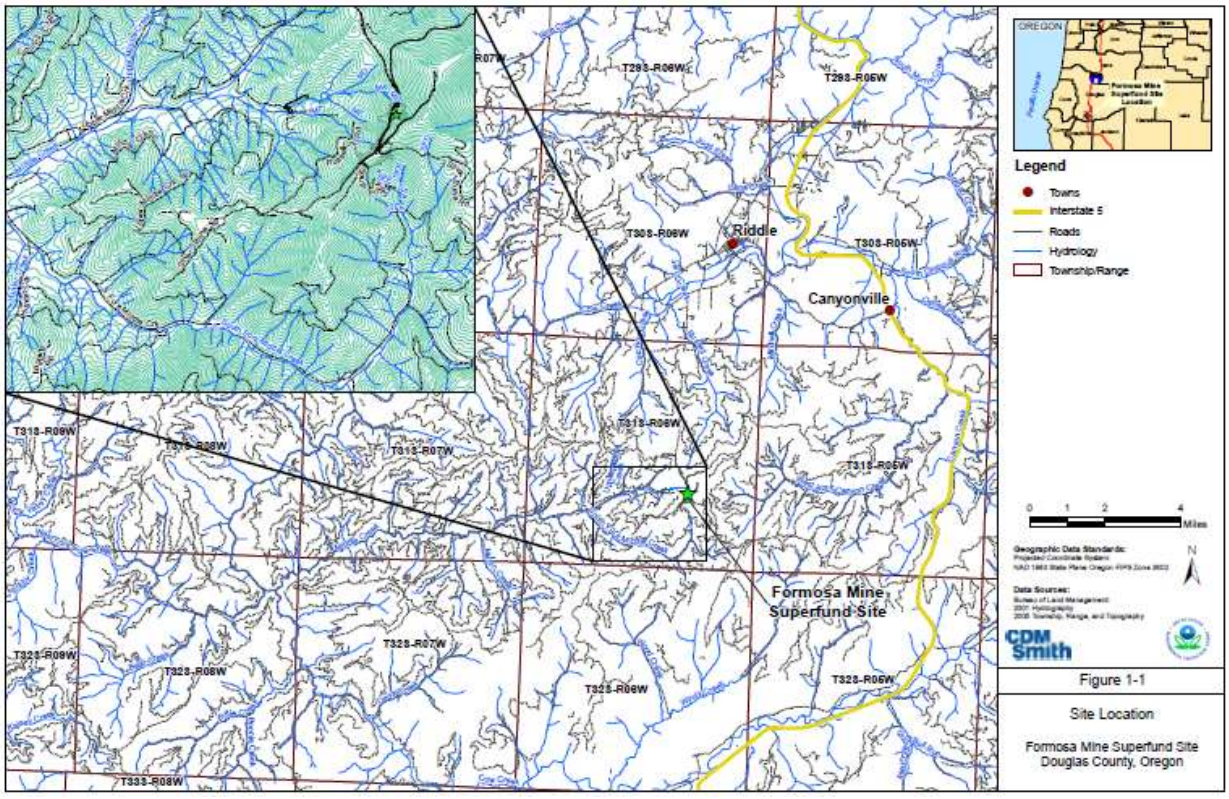

Figure 1- Location of Formosa Mine Superfund Site; map from CDM 2009

Vegetation at the site is typical of the area, consisting mostly of Douglas fir and western hemlock intermixed with Pacific madrone and a few other deciduous tree species. Shrubs are more abundant in

younger stands that have not developed a full canopy. Older growth stands have fewer shrubs and other species amongst them.

Precipitation falls primarily in the winter months from November to March with peak flows occurring in January and February (CDM, 2009). Annual precipitation ranges between 30-55 inches per year at the site. In the winter months, some of this precipitation may fall as snow as this site is located between elevations ranging from about 3200 ft to 3600 ft (CDM, 2009). Visits to the mine made at different times of the year indicate that the seasonal differences in surface water abundance are quite notable, however changes in vegetation are less notable as the species tend to stay green year round.

The Formosa Mine was declared a Superfund Site in 2007. It had been in operation to produce copper, zinc, gold and silver from 1928-1931, 1936-1937 and 1990-1993. During these periods, the underground workings and other infrastructure were built and utilized for mining purposes. The result is a 700 ft deep abandoned mine with waste rock backfilled into portals and adits (CDM, 2009). Waste rock covers a large area around the mine and there are other sites where tailings were illegally disposed (CDM,2009).

Site Features

Figure 2 shows locations of certain site features. The underground workings, adits, seeps and mine waste are all sources of acid rock drainage (ARD) which flows into the headwaters of Middle Fork Creek and South Middle Fork Creek (CDM, 2012). These creeks were habitat for Coho salmon and other aquatic species, however, current conditions have rendered these streams uninhabitable for nearly an 18 mile stretch downstream of the mine (CDM, 2009).

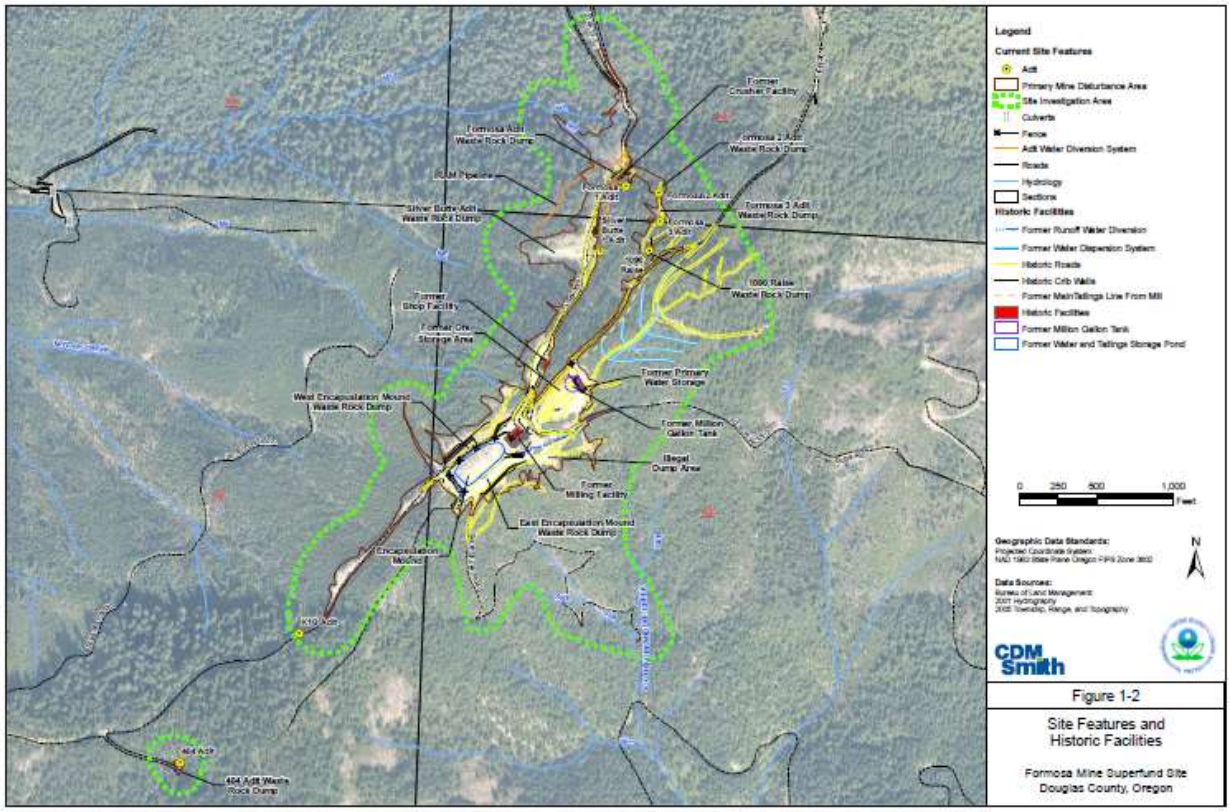

Figure 2- Site features at Formosa Mine Superfund Site; map from CDM 2009.

Several reclamation projects were undertaken between 1993 and 1994, however they did not result in effective treatment or storage of waste rock and tailings (CDM, 2009). Several site features were removed, such as the mill building and processing equipment; mine portals were backfilled, some with limestone and others without; sulfide tailings were removed from upper Middle Creek; and diesel fuel spills were remediated. Despite these efforts, the mine continues to produce millions of gallons of ARD every year (CDM, 2013).

An adit water diversion system was installed between 1993 and 1994. By 1995, it had clogged and flow was observed coming from the surface through the rock fill around the adit where the diversion pipe was built (CDM, 2009). Scaling within the pipes, caused by the high iron content of the drainage water was an ongoing issue that was also quite costly to maintain. Attempts were made to improve the

adit diversion system, however, ARD still enters Middle Creek via groundwater seeps and also from surface waters that flow over and/or through rock fill on the surface (CDM, 2013).

Different Types of Magnetism

Substances are classified according to their response in the presence of an applied magnetic field. It is the ordering of magnetic moments within the structure of different substances that determines their magnetic behavior.

Diamagnetic materials are comprised of atoms with saturated orbital shells. When exposed to an applied magnetic field, a negative magnetization is induced and a repulsive force occurs. Magnetization of these substances is temperature independent. While all substances have diamagnetic properties, some materials have contributions of additional types of magnetism. Figure 3 shows how magnetic moments are ordered differently in paramagnetic, ferromagnetic, anti-ferromagnetic and ferrimagnetic materials.

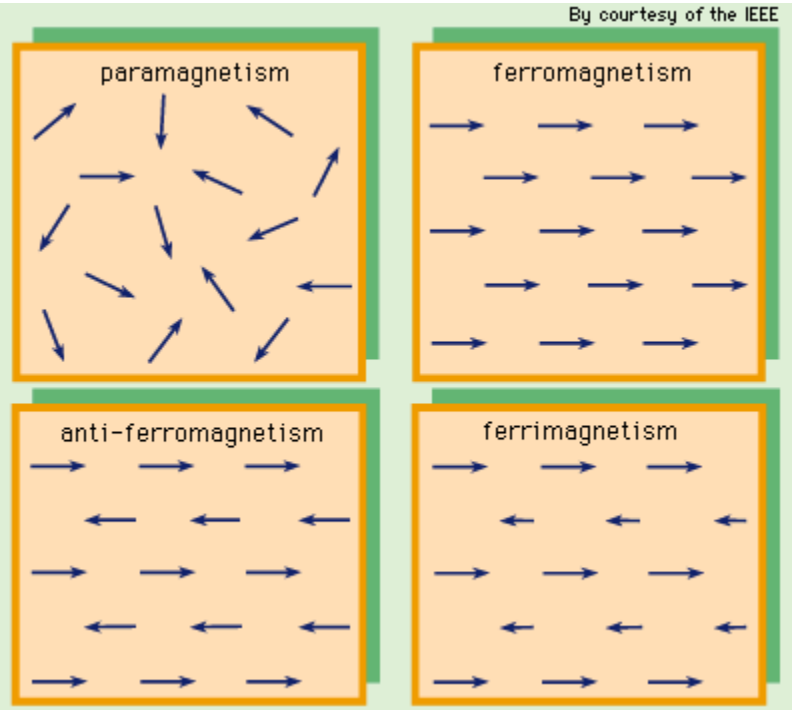

Figure 3- Types of magnetism, http://electrons.wikidot.com/magnetism-iron-oxide-magnetite

Paramagnetic materials have some atoms with unpaired electrons in partially filled orbital shells. This results in positive magnetization in the presence of an applied field, they are attracted to the field. Upon removal of the field, the magnetization of paramagnetic materials returns to zero. The behavior of paramagnetic materials is also temperature and field dependent. Some paramagnetic materials include aluminum, oxygen and iron oxide (FeO).

Ferromagnetic substances are what is typically thought of when referring to magnetic materials. In these materials, there is parallel alignment of magnetic moments in the direction of the Earth's magnetic field. The ordering of magnetic moments is temperature dependent, with spontaneous magnetization observed at lower temperatures. Anti-ferromagnetic substances have equal magnetic moments aligned in opposing directions resulting a net zero magnetization at temperatures below the Neel temperature, which is the temperature above which an antiferromagnetic substance becomes paramagnetic. Ferrimagnetic materials have opposing orientation of magnetic moments. Unlike antiferromagnetic materials, the opposing moments are unequal. Ferrimagnetic materials are paramagnetic above the Curie temperature, at which the magnetic moments of a material become aligned with an applied magnetic field.

Magnetic Parameters of Interest

Presented here are the parameters and measurements of interest to magnetic discrimination of sediments and soils for this study. They include susceptibility, isothermal remanent magnetization and anhysteric remanent magnetization.

Susceptibility measures the ability of a substance to acquire a magnetization in an applied field. Materials that are highly susceptible will attain magnetization at lower fields than those that are less susceptible. Relating this back to the types of magnetism, we would see that ferro- and ferrimagnetic materials would have high susceptibility, anti-ferromagnetic and paramagnetic materials would have

moderate susceptibility several orders of magnitude lower while diamagnetic substances would have extremely low negative susceptibility. Table 1 lists examples of different magnetic materials and their susceptibility.

Table 1- Magnetic behavior and susceptibility, Dearing 1994

Table 2.1 Magnetic behaviour and magnetic susceptibility

Ferromagnetic	Strong positive susceptibility *e.g. pure iron, nickel, chromium*
Ferrimagnetic	Strong positive susceptibility *Some iron oxides and sulphides, e.g. magnetite, maghemite, pyrrhotite, greigite*
Canted antiferromagnetic	Moderate positive susceptibility *Some iron oxides, e.g. hematite, goethite*
Paramagnetic	Weak positive susceptibility *Many Fe-containing minerals and salts, e.g. biotite, olivine, ferrous sulphate*
Diamagnetic	Weak negative susceptibility *e.g. water, organic matter, plastics, quartz, feldspars, calcium carbonate*

Isothermal remanent magnetization (IRM) is acquired using a DC field of various intensities and measures the ability of a sample to retain a magnetization after removal of the applied field. Magnetic response to a DC field reflects a materials magnetic mineralogy and magnetic grain size (Single domain, multi-domain, super paramagnetic and pseudo single domain). For ferrimagnetic materials such as magnetite, we expect that the sample will reach a saturation isothermal magnetization (SIRM) around 300mT. For antiferromagnetic minerals, higher fields are required to reach SIRM. Antiferromagnetic materials, such as hematite have SIRMs around 650-700mT or higher. Paramagnetic and diamagnetic minerals retain no magnetic remanence and therefore do not contribute to a samples SIRM.

Anhysteric remanent magnetization is acquired when a sample within an alternating field is exposed to a small DC field. Fine grained magnetite is particularly sensitive to this type of magnetization. Ratios using ARM values (e.g., ARM/x) are particularly sensitive to variations in magnetic grain size with higher values indicating finer magnetic grain sizes, such as single domain and pseudo-single domain.

Environmental Magnetism

Environmental magnetism uses magnetic techniques to describe or characterize situations where environmental processes affect the transport, transformation and/or deposition of magnetic minerals (Thompson and Oldfield, 1986). To that extent, it can be used to investigate climatic processes, changes in deposition of sediments from atmospheric or fluvial sources or even track the impact of human activity within cities and beyond (Liu et al., 2012; Oldfield et al., 1985; Thompson and Oldfield, 1986; Verosub and Roberts, 1995). The need to better understand the impacts we have on the environment has created demand for quick and inexpensive ways to investigate and monitor air, soil and water. Rock and mineral magnetic techniques provide a possible method to do so where sources of interest have different magnetic signatures than the native sediments and soils. Where this is true, it may provide a timely and cost-effective alternative to costly chemical analysis.

Verosub and Roberts (1995) separate the field of environmental magnetism into three main categories; studying physical process in depositional environments; study of processes that cause variation in magnetic minerals in sedimentary environments; and in-situ processes that alter magnetic mineral content of sediments or soils. The first category is focused on the geologic record. It is used to track variations in the Earth's magnetic field over geologic time scales and investigate properties that might act as proxies for paleoclimatic variation. The second could be used to study inputs of materials from several different sources, for example, atmospheric, fluvial or glacial. The third category uses magnetic techniques to study how sediments might be altered in-situ by biogenic (microbial), pedogenic (soil forming) or authigenetic/diagenetic (mineral altering) processes.

Environmental magnetism has been useful to the field of paleoclimatology. Over time, scientists have developed a well constrained time series for changes in the earth's magnetic field (Lisé-Pronovost et al., 2009; St-Onge et al., 2008) and examined sediment cores for clues of properties that may suggest changes in climatic processes over time (Maher, 2007; Maher and Thompson, 1999). By comparing

records from around the globe, researchers are able to make inferences about past glacial activity (Bloemendal et al., 1992) and the climate conditions that change precipitation (Juyal et al., 2009) and sedimentation patterns (Ariztegui et al., 2001). Combining these records with other paleoclimatic data from ice cores, trees (dendrochronology), and depositional environments (oceans, lakes, etc…) enhances understanding of past climate conditions.

Rock magnetic techniques have also proven useful in elucidating more contemporary processes dealing with source ascription and mapping the extent of deposition of particulates, soils and sediments from various point and non-point sources (Liu et al., 2012; Maher, 2007; Thompson and Oldfield, 1986; Verosub and Roberts, 1995). Magnetic mineralogy or grain size may be related to environmental or anthropogenic processes that enhance the susceptibility of sediments or soils allowing for assessment of affected areas using magnetic measurements where these differences are distinguishable from those of native sediments and soils. Recent research in environmental magnetism tends to focus on its utility as a proxy for mapping pollution from various sources and discriminating sources of pollution in attempt to quantify contributions from different sources (Charlesworth and Lees, 2001; Lecoanet et al., 2003; Liu et al., 2012; Wang et al., 2014).

Wang et al., 2014 use magnetic properties to discriminate soil samples affected by vehicle emissions versus industrial sources. Earlier studies were successful in demonstrating the differences between agricultural soils and urban soils (Hu et al., 2007); mapping the extent of pollutants in river sediments (Chaparro et al., 2008b), polar environments (Chaparro et al., 2008a) and cities (Chaparro et al., 2004; Gautam et al., 2005; Lu and Bai, 2006; Robertson et al., 2003) and tracing atmospherically transported pollutants (Kapička et al., 1999; Shu et al., 2001).

Environmental Magnetism for Monitoring Heavy Metals

There are several sources of heavy metals in the environment, both natural and anthropogenically derived. Application of rock magnetic techniques has proven to be a useful tool in assessing the degree

and extent of heavy metal contamination from a wide range of activities and natural processes (Maher and Thompson, 1999; Oldfield et al., 1985). This section will introduce some of the applications and situations in which environmental magnetism has been successful as a proxy for heavy metal contamination in sediments and soils around the world.

Environmental magnetic techniques have been useful for mapping and assessing the degree and extent of atmospherically transported pollutants and dusts (Heller et al., 1998; Oldfield et al., 1985; Petrovský and Ellwood, 1999; Sapkota and Cioppa, 2012; Shu et al., 2001; Zhang et al., 2011). For example, magnetic minerals found in fly-ash from smelting plants and vehicle emissions are generally coarser in grain size and hence have lower ARM/SIRM ratios (Liu et al., 2012). Dusts created from burning of fossil fuels tend to show correlation between magnetic mineral concentration and heavy metal concentration (Heller et al., 1998; Hoffmann et al., 1999; Shu et al., 2001; Zhang et al., 2011, 2012). Adsorption and incorporation of heavy metals into the structure of magnetic minerals during combustion contribute to this correlation. In many cases where soils have been affected by anthropogenic pollution, magnetic susceptibility can be used to assess the relative degree and extent of contamination (Hoffmann et al., 1999; Kapička et al., 1999; Morton-Bermea et al., 2009; Petrovský and Ellwood, 1999; Shu et al., 2001). Ferromagnetic contributions of anthropogenic origin raise magnetic susceptibility in soils, providing a cost effective alternative to chemical analyses to assess and monitor pollution in urban environments.

Wastewater from various industrial sources is often enriched in heavy metals and may present a source of pollution to rivers, streams and other surface waters. Magnetic studies have proven beneficial in mapping pollution from various sources of wastewater laden with heavy metal contaminants. In one study, authors use magnetic techniques to assess the source of heavy metals from irrigated water versus pesticides and fertilizers (Zhang et al., 2013). The authors find significant correlation between X and the heavy metals Zn, Pb, Cu, Cd, Co, Ni and V, demonstrating that magnetic properties are suitable for evaluating and mapping heavy metal contamination from wastewater irrigation in this area (Zhang et al., 2013).

Lecoanet et al. (2013) use the ratios SIRM/X, IRM-200mT/SIRM, IRM-20mT/SIRM and ARM40mT/SARM to discriminate samples from various sources of pollution in the Crau plain/Berre-Fos basin of southern France. There are clear groupings of samples from specific areas as shown in Figure 4, below with samples in the upper right hand corner of the plot characterized as having higher contributions of coarse ferrimagnetic grains compared to those in the bottom left having less of this material and more paramagnetic minerals (Lecoanet et al., 2003).

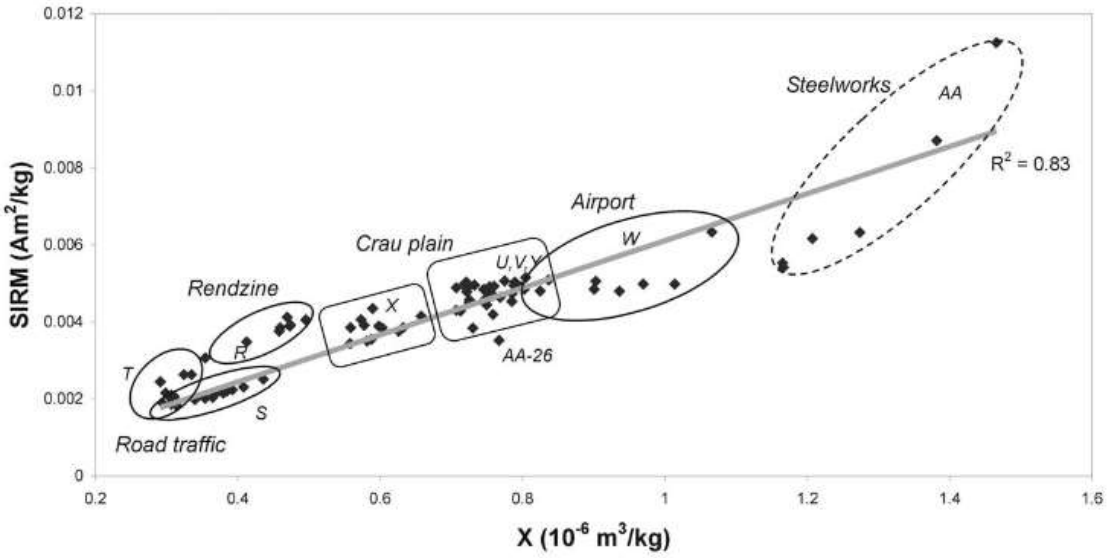

Figure 4- SIRM/X of samples from southern France, Lecoanet et al. (2013)

To date, there have been very few studies focused on the utility of environmental magnetism to monitoring impacts from mining processes. The majority of these studies have been overseas. One study, done in Spain used magnetic gradient mapping to assess infilling processes in Portman Bay (Peña et al., 2013). Later studies in the same bay found significant relationships between magnetite content and heavy metals Pb, Cu and As (Gómez-García et al., 2015).

Why Environmental Magnetism for Formosa?

There are thousands of abandoned mines scattered throughout the US and other countries, many of which are not mapped or known. Even at Formosa, the full extent of the contamination has not been determined, although it is estimated that over 75 acres are affected. Furthermore, downstream effects are only monitored up to a certain distance from the mine and are not necessarily monitored over time in different seasons. The mine was in operation during two periods, one in the 1930's and more recently in the late 90's. It is possible that magnetic measurements allow for a quick and easy assessment of variations in soil properties that could be linked to periods of mining such as magnetic grain size and concentration of certain diagnostic magnetic minerals.

The question of interest is whether or not there actually are specific magnetic properties that can be used to assess the extent of anthropogenic pollution at this site and if so, which ones. If this is the case, then sediments downstream from the site and outside of the affected area will have significant differences in magnetic properties compared to samples from the mine. Whether or not these properties are related to heavy metal concentrations is also of interest for mapping hot spots to target for remediation purposes. The specific question becomes which properties, if any, are useful in distinguishing sediments from the mine from sediments found downstream from the mine in Middle Fork Creek.

Materials and Methods

The sampling design is based on access to site features and otherwise is random but distributed to capture variability as a function of elevation and proximity to drainage routes. The main site is accessible via gravel roads that lead up to the encapsulation mound and adit diversion project. Decommissioned roads allow for access to downhill areas to the west and south of the encapsulation mound. Middle Creek was sampled along roadways that are accessible from the Cow Creek Bi-way that travels up Cow Creek to Middle Creek from Riddle, OR. The sampling sites are shown in Figures 5 and 6.

Surface samples were taken from the area surrounding the main features of the mine and from Middle Creek, downstream from the mine. Bulk samples are taken prior to wet sieving. Sediments are then treated with Calgon, a dispersing agent that helps break apart aggregated sediments, and deionized water for subsequent separation. The sediments are then wet sieved using two different mesh sizes; 63µm and 20µm. The result is four different 'fractions' for each sample; the bulk fraction which contains all particle sizes, over 63µm, 20-63µm and under 20µm.

Sediments are dried in an oven at 40C for up to approximately 10 days, the smaller fractions taking longer to dry. These samples were then subsampled, measured for mass and placed in 8cm3 plastic cubes that fit into a track made for taking discrete measurements in the magnetometer. These subsamples were then subjected to a series of measurements for magnetic susceptibility (BartingtonMS2), ARM, IRM (2G Enterprises superconducting rock magnetometer) and metal concentrations using a portable X-Ray Flourescence instrument (Bruker pXRF).

Sampling

Surface samples of soils and sediments around the abandoned mine and downstream in Middle Creek were obtained with sporks, using the serrated side to disturb the surface and the spoon side to scoop it into Ziploc bags. These bags were then labeled with GPS coordinates that were stored as waypoints in a handheld Garmin GPS instrument based on the WGS84 Datum in units of decimal degrees. These can be

seen in Figure 5 which is a terrain view of the area sampled and Figure 6, a satellite view of the same area.

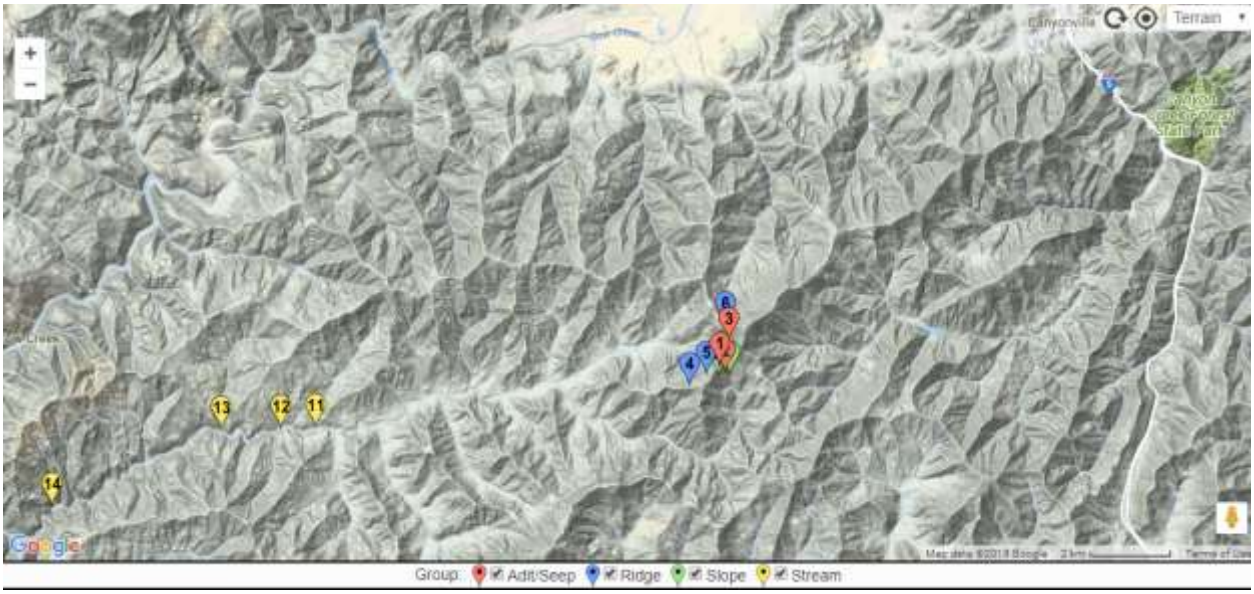

Figure 5- Map of all points sampled

Figure 6- Satellite map of areas sampled

The Formosa Mine points are tightly clustered at the scale in the Figures above. For a more detailed view of these points, they were mapped at a scale of 200m in both terrain (see Figure 7) and satellite view (see Figure 8).

Figure 7- Formosa points in terrain view at 200m scale; red flags=samples from the adit/seeps, blue flags=samples from the ridge and green flags=samples from the slope

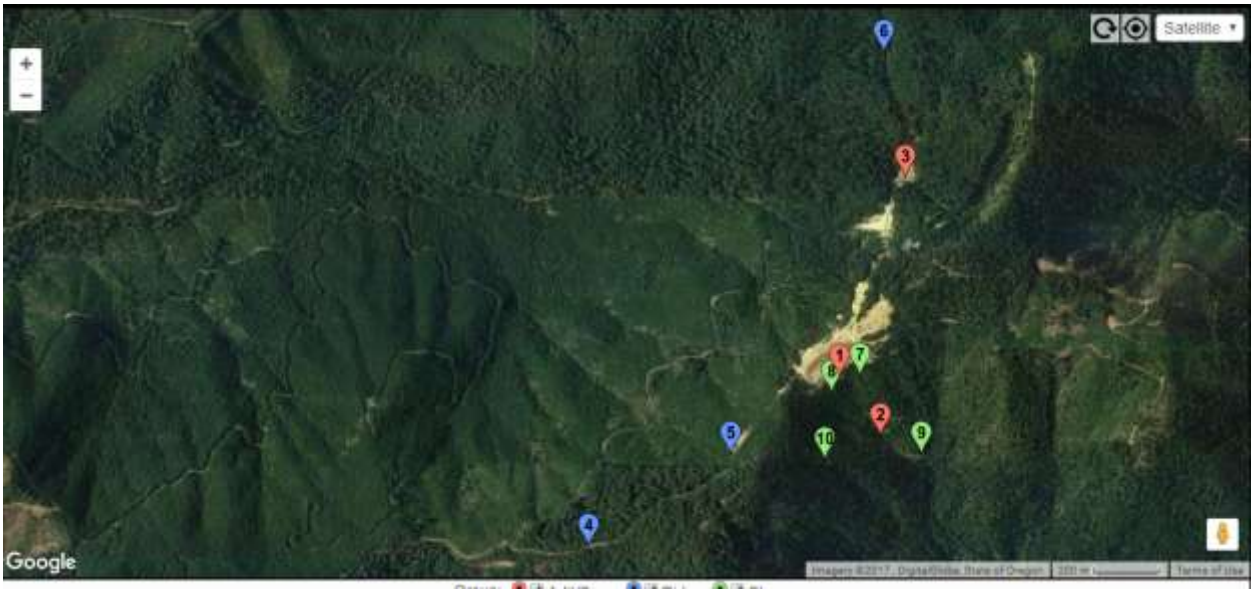

Figure 8-Formosa points in satellite view at 200m scale; red flags=samples from the adit/seeps, blue flags=samples from the ridge and green flags=samples from the slope

Samples from the mine were grouped according to the feature or similarity of terrain they were obtained from with four groups in total; adit/seep, stream samples from Middle Creek, samples taken along the ridge and samples taken from the slope leading down to the east of the encapsulation mound. There are 14 samples in total described below and identified in Table 2.

Table 2- Mapped sample number, corresponding Formosa ID and group designation for all points

Sample Number	Formosa ID	Group
Sample 1	FM2	Adit/Seeps
Sample 2	FM5	Adit/Seeps
Sample 3	FM13	Adit/Seeps
Sample 4	FM10	Ridge
Sample 5	FM11	Ridge
Sample 6	FM12	Ridge
Sample 7	FM1	Slope
Sample 8	FM3	Slope
Sample 9	FM7	Slope
Sample 10	FM8	Slope
Sample 11	MC1	Stream
Sample 12	MC2	Stream
Sample 13	MC3	Stream
Sample 14	MC4	Stream

Sample 1 was taken from a flow path, along the side of the road heading down to the headwaters of Cow Creek. Sample 2 was taken adjacent to a seep on the slope to the east of the encapsulation mound. Sample 3 is from the adit, along the road leading up to the encapsulation mound. These three samples are grouped together and represent samples from areas that are exposed to constant drainage from sources of acid rock drainage.

Samples 4, 5 and 6 were taken along the ridge that separates Middle Creek from Cow Creek. These three samples were taken at elevations ranging from approximately 1000 to 1050m a.s.l. along the road that runs along the ridge which is covered with waste rock.

Samples 7, 8, 9 and 10 were taken from the eastern slope of the site. This slope is steep but has a road that runs part way down the hill making it far more accessible than the slope leading into Middle Creek.

The remaining 4 samples were taken from Middle Creek at spots where the stream was accessible on foot. The road leading along the creek up to Formosa Mine had been blocked by a landslide approximately 2 months prior to the sampling date and a small area along the eastern slope down into the creek had been burned the previous summer (2014).

MS2B Susceptibility Measurements

Depending on the abundance of each fraction, between 0.4 and 2g of sediment were prepared for susceptibility and other magnetic measurements. Sediment was weighed and enclosed in cellophane which was then placed between layers of cotton swab (as filler) in $8cm^3$ containers designed to fit in the Bartington MS2 Susceptibility Meter. Measurements were taken at both low (0.47kHz) and high (4.7 kHz) frequencies.

Isothermal Remanent Magnetization

Samples were subjected to an instantaneous magnetization imparted using a pulsed DC field then their remanence was measured in the magnetometer. IRM acquisition was a stepwise process with the first pulse at a strength of 20mT increasing to 1000mT through a series of measurements. The steps that were measured for acquisition of a magnetization were 20mT, 40mT, 60mT, 100mT, 200mT, 300mT, 500mT, 700mT and 1000mT. These samples were then demagnetized and then measured after AF demagnetization of 10mT, 15mT, 20mT, 25mT, 30mT, 35mT, 40mT, 50mT, 80mT and 100mT.

Anhysteric Remanent Magnetization

For ARM measurements, samples are subjected to decreasing alternating fields (AF) starting at 100mT in the presence of a constant direct current field of low intensity, in this case 0.5 mT. Remanent

magnetization was measured after demagnetization at peak AF of 0mT, 10mT, 15mT, 20mT, 25mT, 30mT, 35mT, 40mT, 50mT, 60mT, 80mT and 100mT.

XRF measurements for Heavy Metals

XRF measurements were taken using the Bruker portable XRF unit. A very small amount of sample is needed for each measurement but samples must be well mixed to obtain representative measurements for each fraction. Samples were placed in sampling containers made from a narrow piece of PVC (~0.5 inch diameter) with pieces of cellophane stretched over the top and bottom then secured with an elastic band. Samples were measured every 5 seconds for 1 minute and 30 seconds then reported as an average and recorded in the instrument database.

Analysis

Susceptibility was normalized by mass then tabulated for each sample. Average, maximum and minimum values were determined for each particle size and these values were added to Table 1. Anhysteric remanent magnetization and isothermal remanent magnetization were converted from the units reported by the magnetometer (emu cm-3) to SI units (Am-1). Since Am-1= 10-3emu, this conversion is done by multiplying the emu cm-3 by 1000. The data was then adjusted for volume to obtain the total magnetic dipole moment (m) by multiplying the raw number obtained from the magnetometer by the volume of the container used to contain the sediments (8x10-6m3). After correcting for volume, the data are normalized by mass to obtain mass specific magnetization (σ) by dividing m by the mass of the sample in kg.

Curves were plotted for ARM and IRM demagnetization by plotting the mass specific magnetization calculated for each step: 10mT, 15mT, 20mT, 25mT, 30mT, 35mT, 40mT, 50mT, 80mT

and 100mT for IRM and 10mT, 15mT, 20mT, 25mT, 30mT, 35mT, 40mT, 50mT, 80mT and 100mT for ARM. The IRM acquisition curve was plotted from measurements taken after exposing samples to magnetic fields of increasing strengths at 20mT, 40mT, 60mT, 100mT, 200mT, 300mT, 500mT, 700mT and 1000mT, then measuring their magnetization in the magnetometer.

IRM acquisition plots were created by plotting the IRM measured by the magnetometer after exposure of sediments to increasing strengths of an instantaneous magnetic field. Acquisition ratios were plotted for each step in the IRM data to determine the strength of field needed to saturate a sample. These were obtained by dividing the magnetization acquired at each step by the saturation IRM, which is generally taken as the magnetization measured after exposure to a field strength of 1000mT. For example, the IRM acquired at 20mT was divided by that measured at 1000mT, and so forth.

Pearson correlation coefficients and the associated p-values were calculated in R software using the variables X, SIRM/X and the concentrations for heavy metals Ti, V, Mn, Fe, Ni, Cu, Zn and As.

Samples were grouped based on where they were taken, creating 4 groups with 3-4 samples each. They were classified as being either ridge, slope, adit/seep or downstream samples. Boxplots were plotted in R and used to explore differences in median and quartile ranges of each group of samples for X, SIRM, SIRM/X, and the heavy metal concentrations. Boxplots are a non-parametric tool for visualizing the dispersion and skewness of a sample population. The upper and lower extensions of the boxes, the whiskers, show the maximum and minimum values of the populations. The upper line of the box marks the 75% quartile; the bottom line of the box marks the 25% quartile and the solid line across the box marks the median. Looking at the spread between different groups allows for assessment of whether or not there are differences between them. Where there is no overlap between spreads, there is a difference between the groups. Where there is overlap of spreads but not the medians, there is a likely difference between groups. Where boxes overlap with both medians, there is no difference between groups. For the purposes of this study, the author considers the differences where there are no overlaps between the spreads to be significantly different.

Heavy metal concentrations for particle sizes over 63μm and the bulk fraction were not collected and hence are not included in the analysis.

Mapping

The GPS points were imported into an online mapmaker, EasyMap and then mapped to Google Map base layers for terrain features and satellite imagery. The terrain images show relief while the satellite images give detail on land cover in terms of areas that are vegetated versus those that have been recently disturbed by fire and/or logging activities.

Results

Bulk Fraction

The average susceptibility for samples in the bulk fraction is 9.0x10-3m3/kg with the highest susceptibility found in the Middle Creek samples (1.9x10-2m3/kg at MC1) and the lowest from Formosa Mine (7.9x10-3m3/kg at FM5).). IRM acquisition curves for these samples indicate that most samples are saturated at approximately 300mT (see Figure 9). Likewise, they are generally demagnetized by a backfield of 300mT (see Figure 10). In this fraction, sample FM1 has much higher intensity compared to other samples.

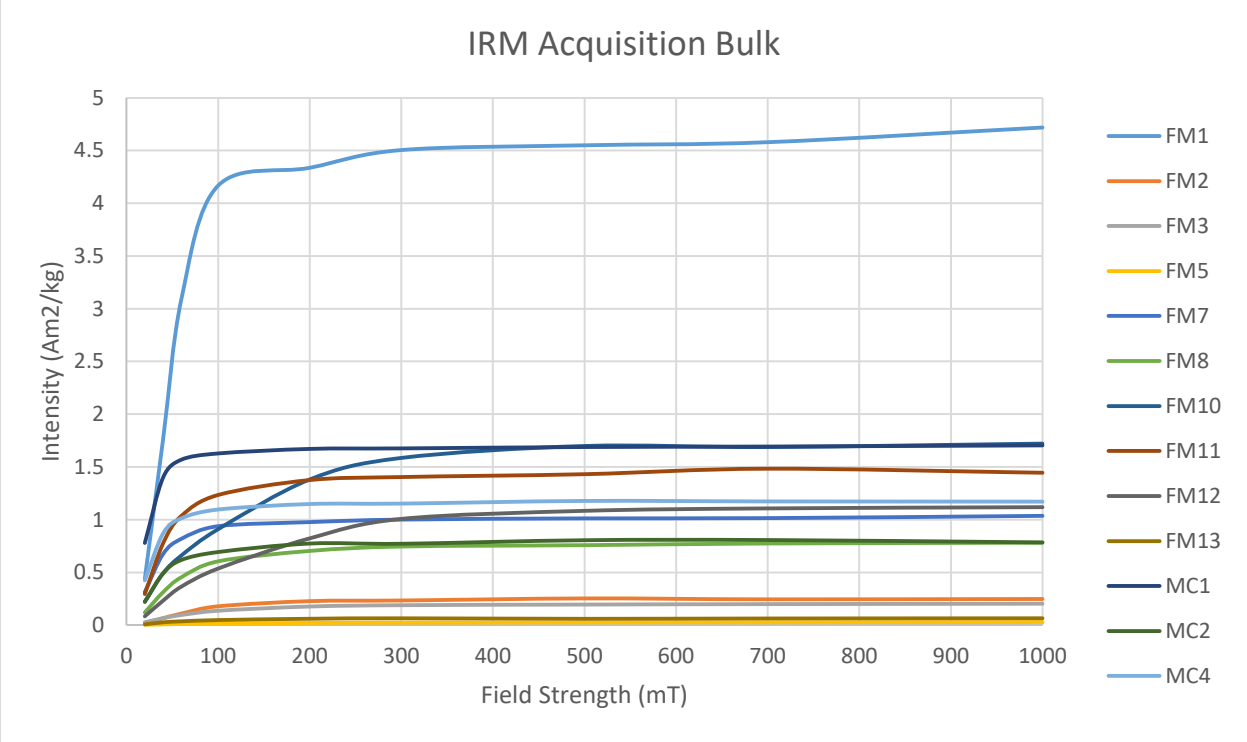

Figure 9- IRM acquisition curves for each sample in the bulk fraction

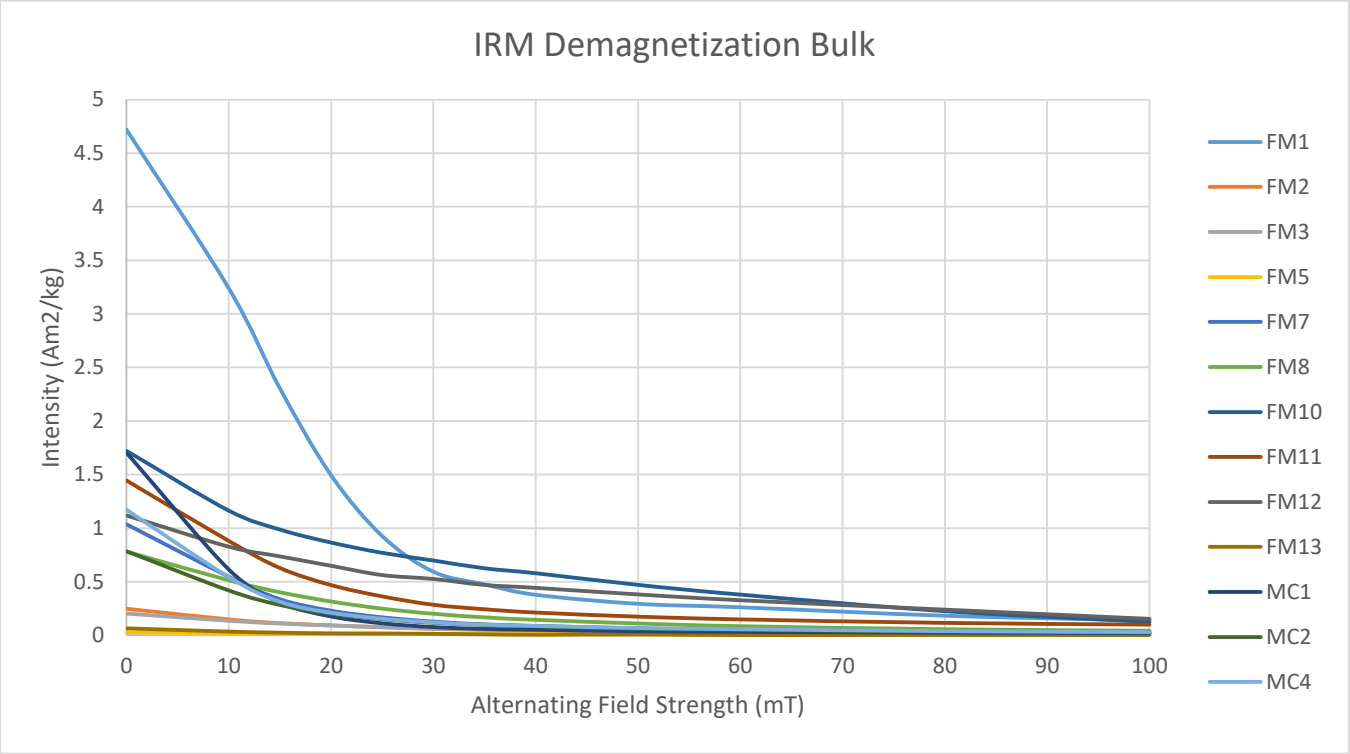

Figure 10- IRM demagnetization curves for all samples in the bulk fraction

There are significant differences in susceptibility between samples taken near adits/seeps and all other groups (see Figure 11). There is also significant difference in susceptibility of downstream samples compared to all other groups. The ridge and slope samples do not show significant variability. A similar trend is observed for SIRM/X in this fraction (see Figure 12).

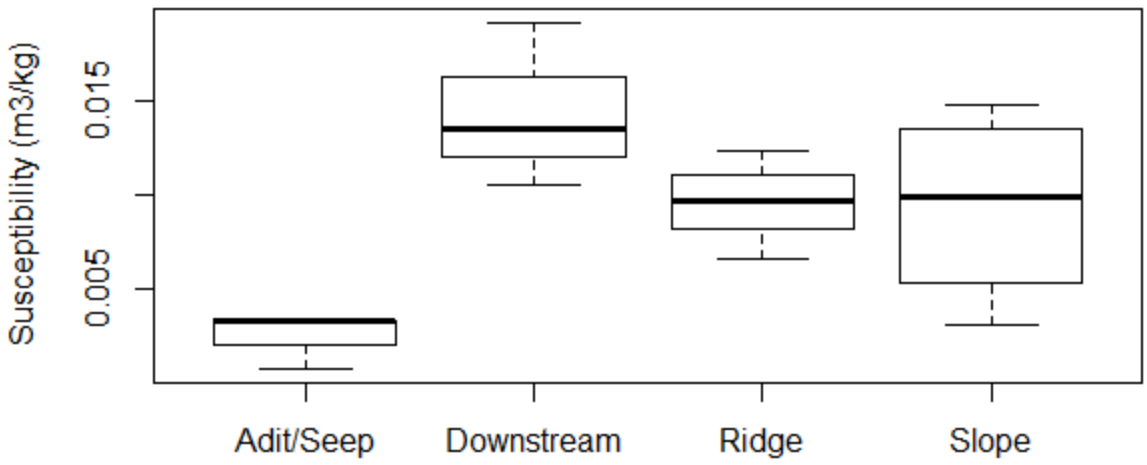

Figure 11-Box and whiskers plot of susceptibility for grouped samples in the bulk fraction

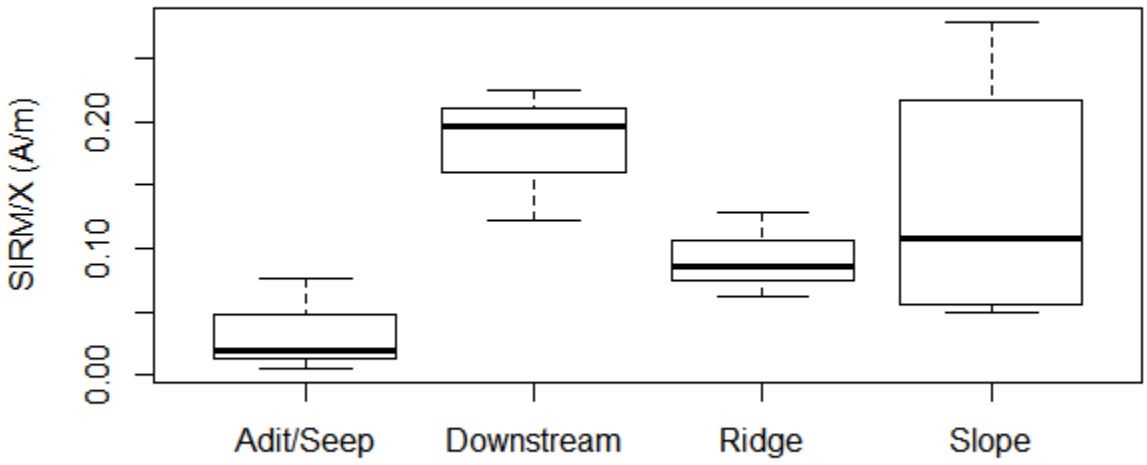

Figure 12-Box and whiskers plot of SIRM/X for grouped samples in the bulk fraction

Over 63µm Group

Samples in the >63m fraction have susceptibilities that range between 1.3x10-3m3/kg (FM5) to 1.7x10-2m3/kg (MC2). Samples FM2, FM5 and FM13 have steeper acquisition curves compared to other samples (see Figure 13). For samples over 63m, FM12 is an outlier, with intensity much greater than the other samples at all field strengths. Again, for this fraction, FM1 has higher intensity of IRM than the other samples.

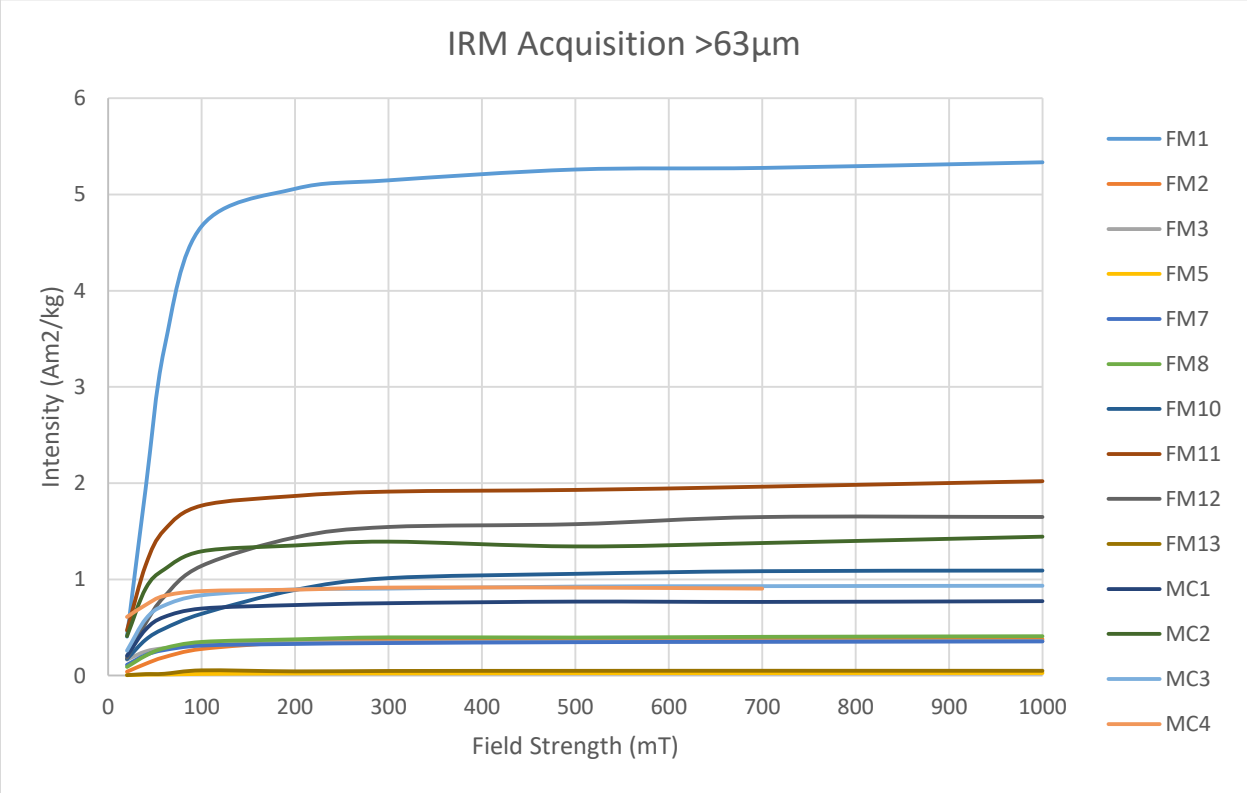

Figure 13-IRM acquisition curves for all samples in the over 63µm fraction

The IRM demagnetization curves show that all samples are near completely demagnetized by a backfield of approximately 300mT (see Figure 14).

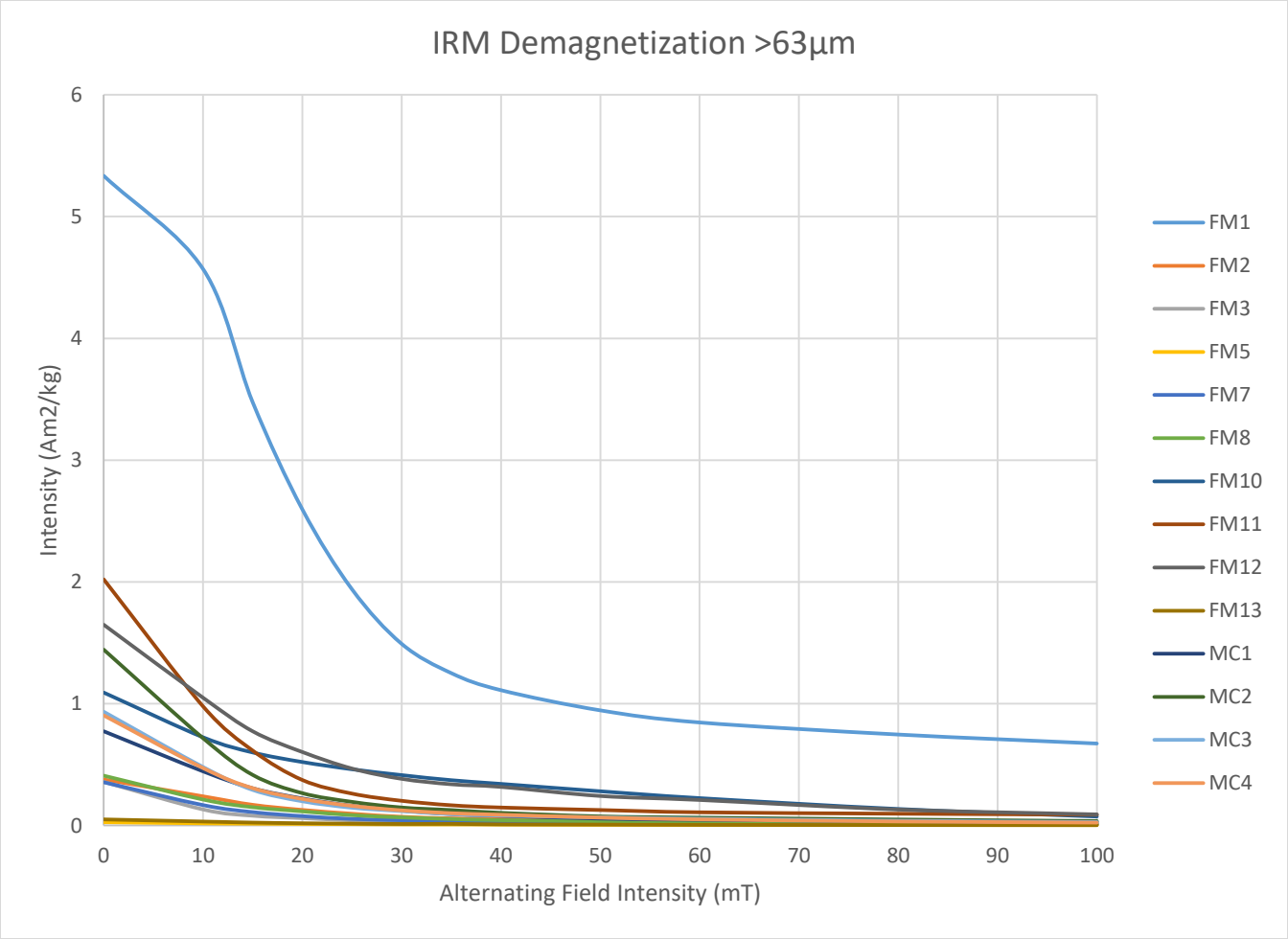

Figure 14- IRM demagnetization curve for all samples in the over 63µm fraction

There are significant differences in susceptibility of the samples taken near adits/seeps compared to all other groups (see Figure 15). There is suggestive difference in susceptibility between samples taken from the slope and those from the ridge. The plots show no significant difference in susceptibility of the downstream samples compared to those taken from the ridge.

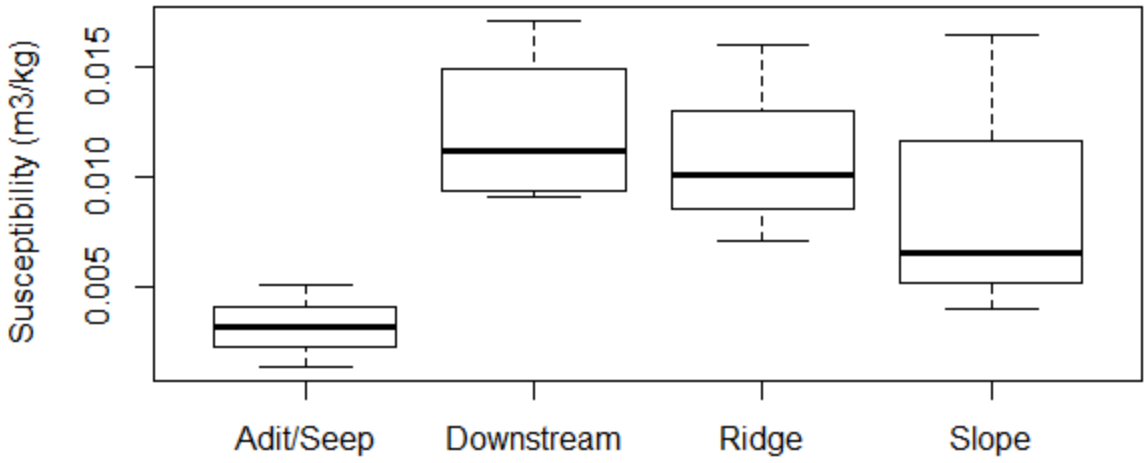

Figure 15-Box and whiskers plot of susceptibility for grouped samples over 63µm

SIRM/X has significant differences between Adit/Seep, Downstream and the Ridge (see Figure 16). The ridge displays no significant difference with the slope group however the spread of data from this group is much greater than that of the other groups.

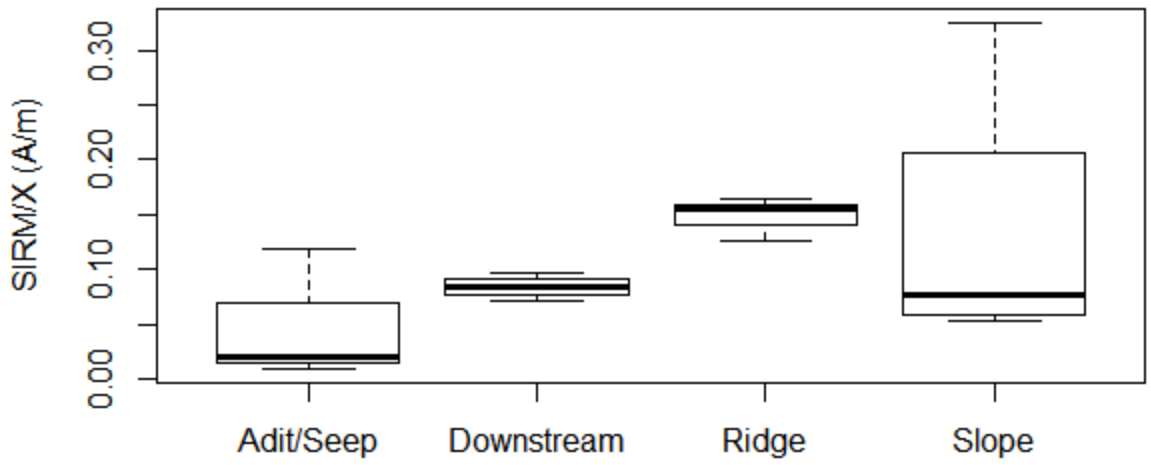

Figure 16-Box and whiskers plot of SIRM/X for grouped samples in the over 63µm fraction

20 to 63m Fraction

Susceptibility for the 20-63µm fraction ranges from 2.1x10-3m3/kg (FM3) to 1.5x10-2m3/kg (MC4). From Figure 17, we see that there is a fairly steep increase in intensity with increasing DC field during IRM acquisition experiments for the majority of samples. Samples FM10 and FM12 show a lesser response to increasing field intensities, indicating that they have a higher coercivity that the other samples . Additionally a few samples (FM2, FM5 and FM13) having much lower intensity measurements than the rest.

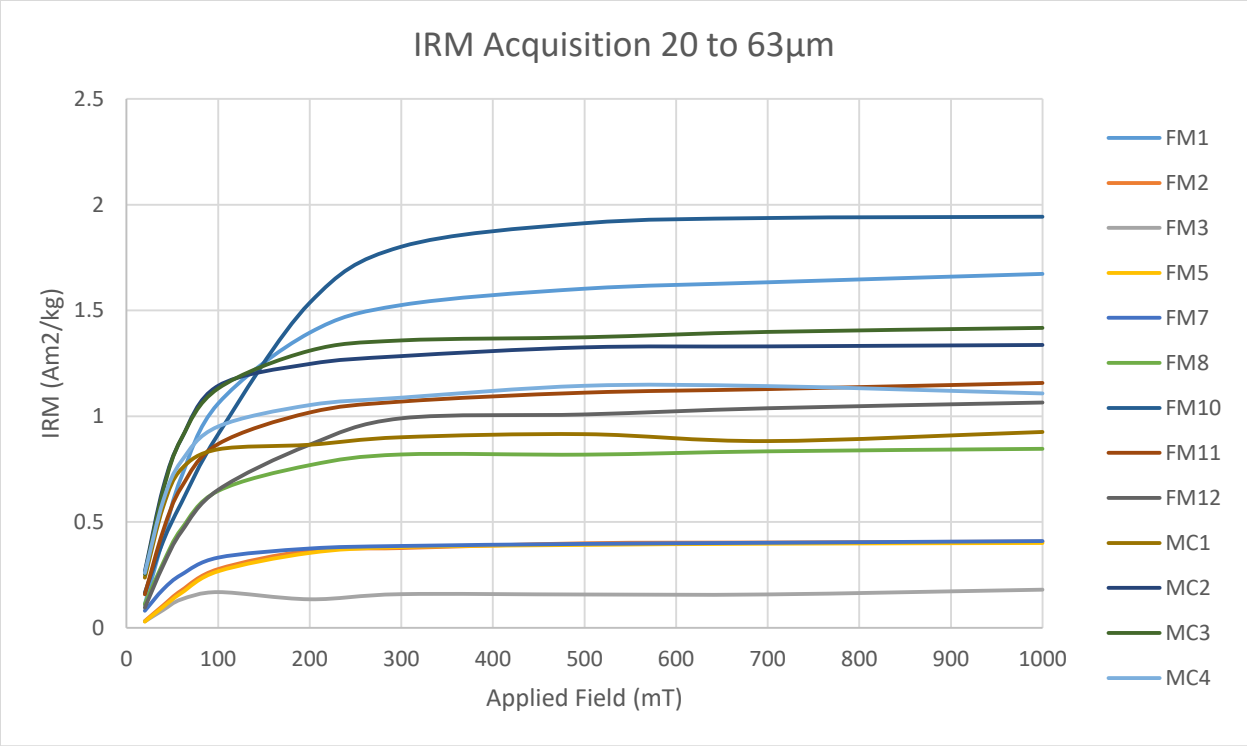

Figure 17-IRM acquisition curves for all samples between 20 and 63µm

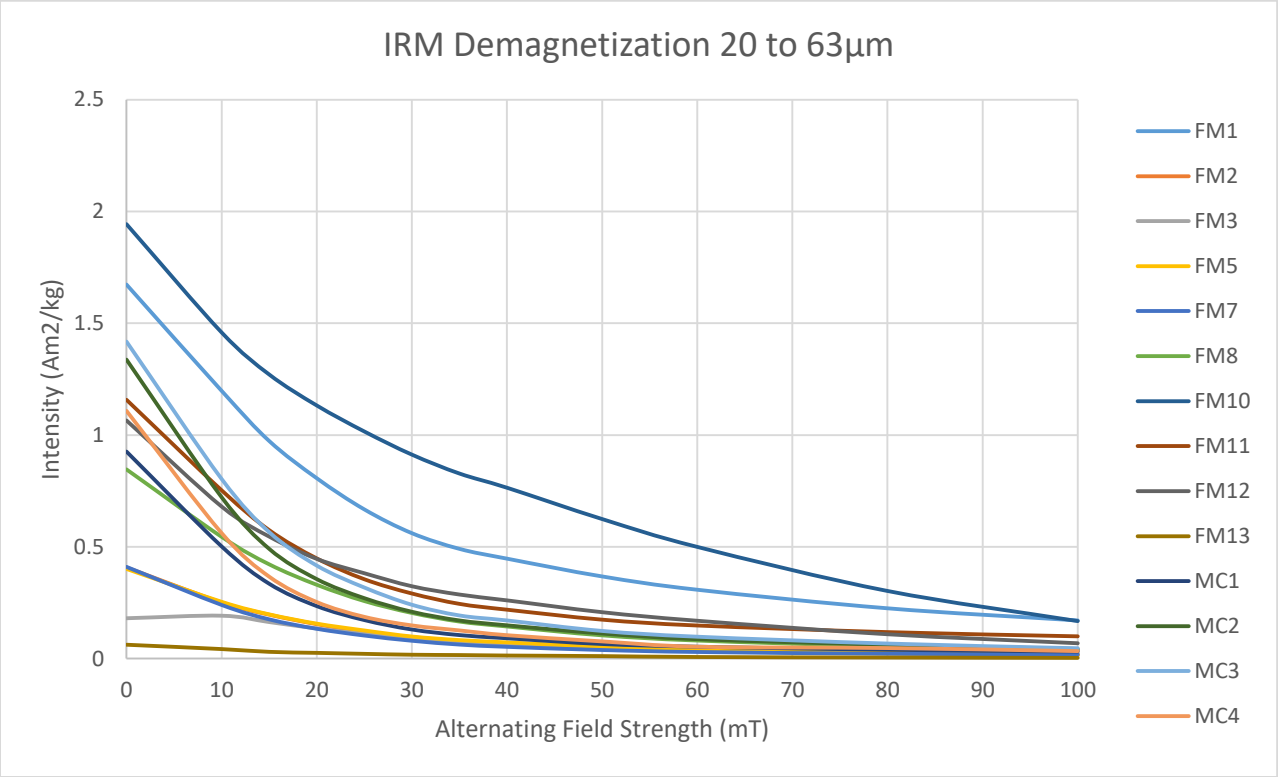

Figure 18-IRM demagnetization curves for all samples between 20 and 63µm

Susceptibility of the downstream samples in this fraction, is significantly different than that of the samples from adit/seep samples, the ridge and the slope samples (see Figure 19). The adit/seep samples are not significantly different from those collected from the slope.

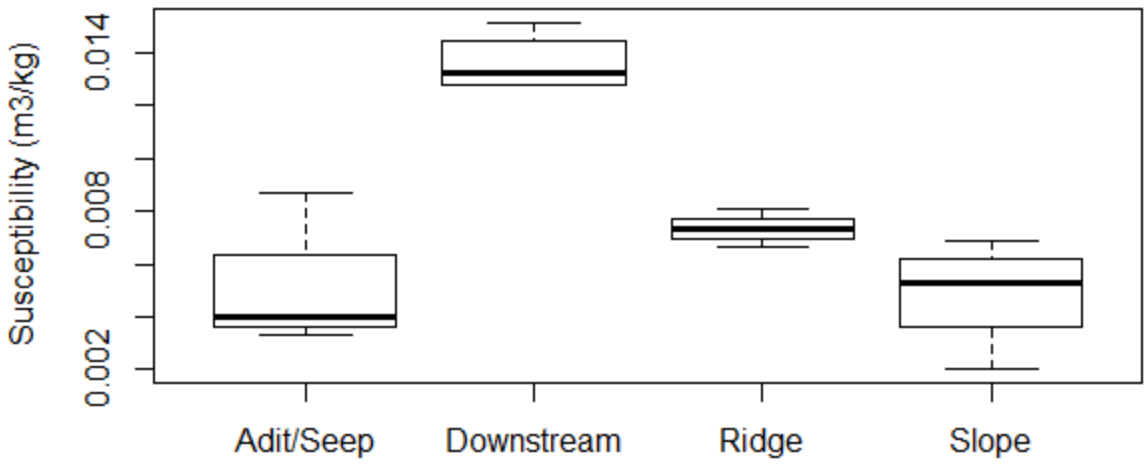

Figure 19- Box and whiskers plot of susceptibility for grouped samples between 20-63m

The boxplots in Figure 20 indicate that SIRM/X is significantly different from those taken from adit/seeps as well as the downstream samples. There is suggestive difference between the samples from the ridge and those of the slopes and no significant difference in SIRM/X between samples from the adit/seeps and downstream samples.

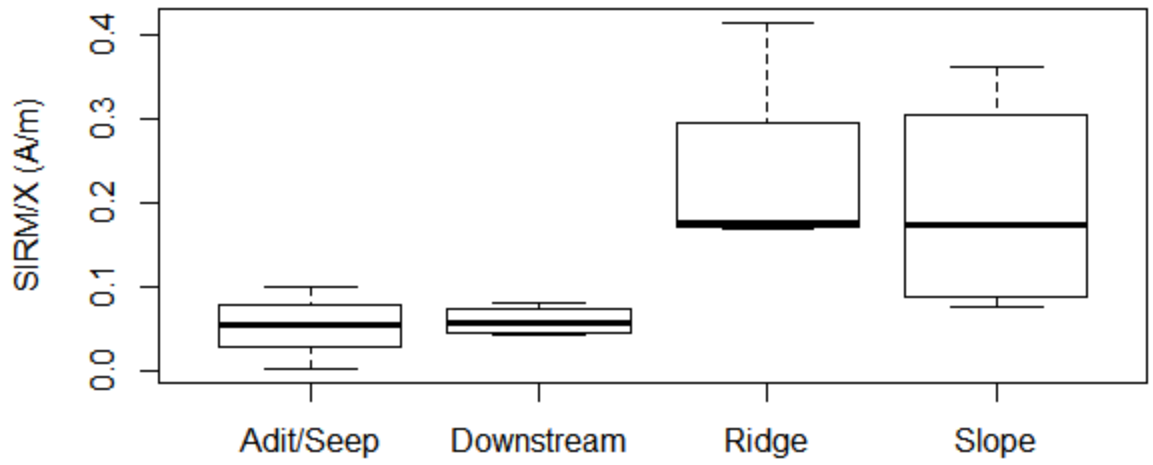

Figure 20-Box and whiskers plot of SIRM/X for grouped samples between 20-63m

The concentration of Fe (iron) in the samples from the adit/seeps varies significantly from that of all other groups (see Figure 21). There is also significant variation between samples from the ridge and slope and downstream samples. The ridge and the slope do not have significant difference in the concentration of Fe. For Ti (titanium), there is significant difference between samples taken from the ridge and those taken downstream however there is no significant difference between the samples in the other 3 groups. Concentration of V (vanadium) are not significantly different between any groups, however the range of concentrations of V in samples from the adit/seep is much more variable than that of the other groups. Concentrations of Mn (manganese) are significantly different between samples taken from the slope and all other groups. There is suggestive significant difference between samples from the ridge and those taken downstream. There is no significant difference between samples taken from the adit/seep and those from downstream. The concentration of Zn (zinc) is significantly higher in the samples from the adit/seep than those from all other areas. Concentration of Zn from the slope is significantly lower than that of the other groups. There is no significant difference between samples from

the ridge and those taken downstream. There is significant difference in the concentration of Cu (copper) between samples taken from the adit/seeps and those from downstream and the slope. There is evidence of significant difference between samples taken from the slope and ridge and those taken from downstream. Concentrations of Ni (nickel) in samples from downstream are significantly higher than those from the ridge. There is little to no Ni in samples from the adit/seeps and the ridge. There is little to no As (arsenic) in samples taken from downstream. Concentrations of As from the mine are significantly higher is samples taken from the adit/seeps compared to those taken from the ridge and slope. There is no significant difference in concentration of As in samples taken from the slope and the ridge.

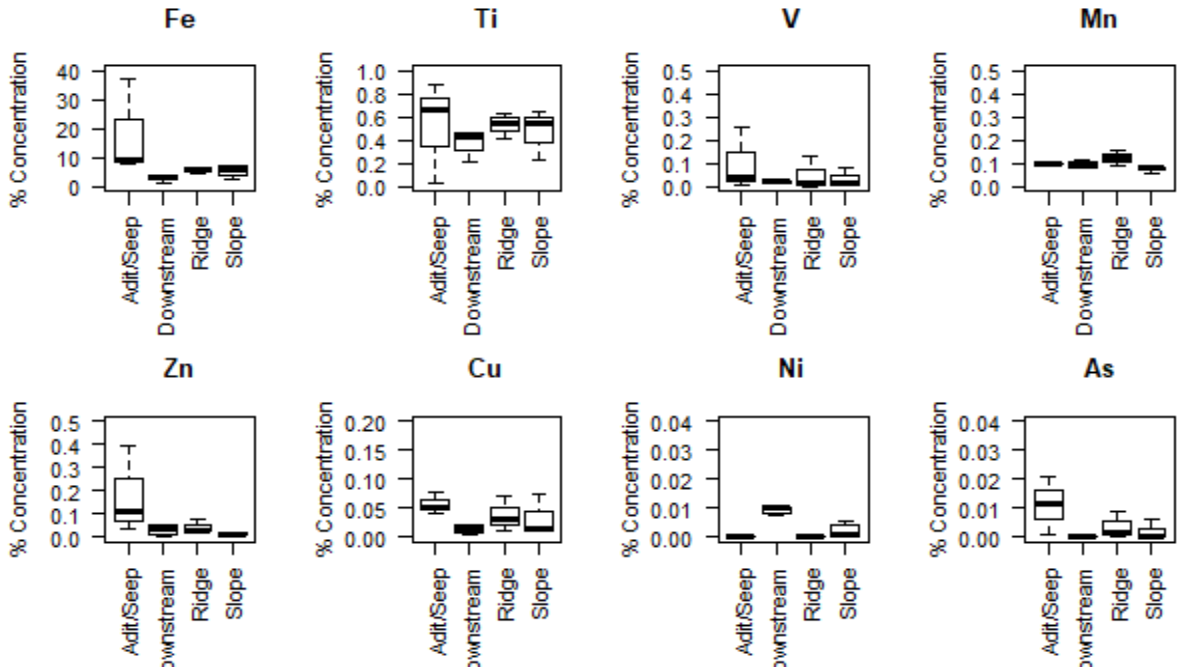

Figure 21- Heavy metal concentrations for samples between 20 and 63µm

Regression coefficients for magnetic properties and heavy metal concentrations are presented in Table 3. There are strong correlations between some heavy metals but none between magnetic properties and heavy metal concentrations.

Table 3- Regression coefficients for correlations between X, SIRM/X and heavy metal concentrations for all samples between 20 and 63µm

	Xlf	SIRM/X	Ti	V	Mn	Fe	Ni	Cu	Zn	As
Xlf	1	-0.3214	-0.39044	-0.35958	0.188589	-0.09298	0.846678	-0.33842	0.019792	-0.21762
SIRM/X	-0.3214	1	0.487864	0.047611	0.236615	-0.33824	-0.30791	0.210089	-0.41894	-0.19024
Ti	-0.39044	0.487864	1	0.648927	0.222574	-0.40988	-0.19675	0.16452	-0.50283	-0.12928
V	-0.35958	0.047611	0.648927	1	-0.13411	-0.05886	-0.32017	0.495499	-0.09774	0.448862
Mn	0.188589	0.236615	0.222574	-0.13411	1	0.058601	-0.03283	0.035699	0.049504	-0.04008
Fe	-0.09298	-0.33824	-0.40988	-0.05886	0.058601	1	-0.32313	0.587494	0.957546	0.820977
Ni	0.846678	-0.30791	-0.19675	-0.32017	-0.03283	-0.32313	1	-0.55955	-0.25142	-0.47012
Cu	-0.33842	0.210089	0.16452	0.495499	0.035699	0.587494	-0.55955	1	0.594516	0.846153
Zn	0.019792	-0.41894	-0.50283	-0.09774	0.049504	0.957546	-0.25142	0.594516	1	0.791901
As	-0.21762	-0.19024	-0.12928	0.448862	-0.04008	0.820977	-0.47012	0.846153	0.791901	1

For the 20 to 63m fraction there is significant correlations between X and the concentration of Ni (see Table 4). There are significant correlations between some of the heavy metals including Ti and V, Cu and Fe, Cu and Ni, Cu and Zn, Zn and Fe, As and Fe, As and Cu and As and Zn.

Table 4- p-Values for Pearson correlations between X, SIRM/X and heavy metal concentrations for all samples between 20 and 63µm

	Xlf	SIRM/X	Ti	V	Mn	Fe	Ni	Cu	Zn	As
Xlf	NA	0.262496	0.16752	0.206675	0.518485	0.751883	0.000134	0.236603	0.946457	0.454844
SIRM/X	0.262496	NA	0.076771	0.8716	0.415386	0.236862	0.284173	0.470972	0.135968	0.514767
Ti	0.16752	0.076771	NA	0.012043	0.444378	0.145529	0.500206	0.574091	0.066857	0.659588
V	0.206675	0.8716	0.012043	NA	0.647599	0.841569	0.26444	0.07159	0.739589	0.107409
Mn	0.518485	0.415386	0.444378	0.647599	NA	0.842268	0.911277	0.903568	0.866537	0.891794
Fe	0.751883	0.236862	0.145529	0.841569	0.842268	NA	0.259796	0.027162	7.71E-08	0.000319
Ni	0.000134	0.284173	0.500206	0.26444	0.911277	0.259796	NA	0.037472	0.385898	0.089823
Cu	0.236603	0.470972	0.574091	0.07159	0.903568	0.027162	0.037472	NA	0.024944	0.000136
Zn	0.946457	0.135968	0.066857	0.739589	0.866537	7.71E-08	0.385898	0.024944	NA	0.000736
As	0.454844	0.514767	0.659588	0.107409	0.891794	0.000319	0.089823	0.000136	0.000736	NA

Under 20m Fraction

For the smallest fraction (<20µm) mass susceptibility ranges from 9.7x10-4m3/kg (FM3) to 2.1x10-2m3/kg (MC4). The IRM acquisition curves in Figure 22 show some variation in the rate of

acquisition for each sample. As in the case of the 20-63m particle size, we see that there is a fairly steep curve for the majority of samples, with a few samples having much lower intensity of IRM (FM1, FM10 and FM12). These are samples FM2, FM5 and FM13.

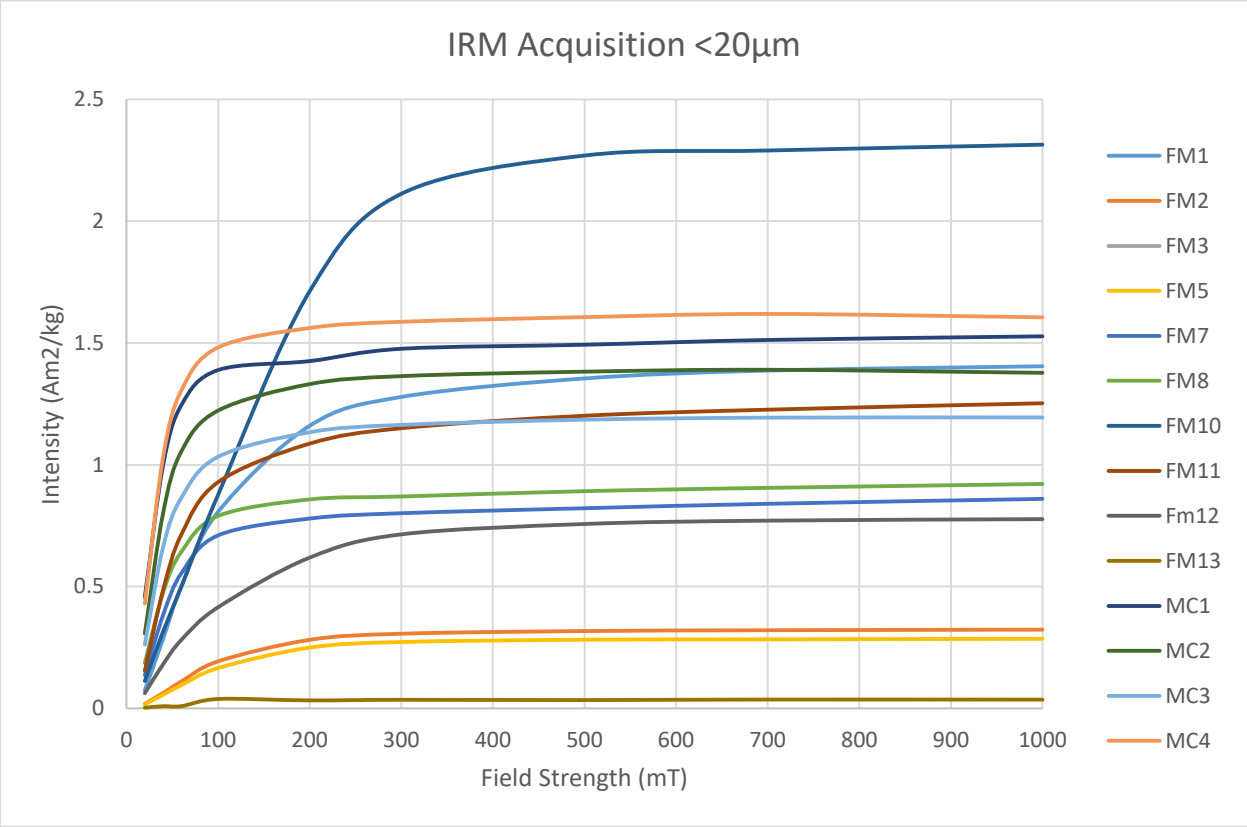

Figure 22- IRM acquisition curves for all samples under 20µm

The demagnetization curves show that samples are generally demagnetized by a field strength of approximately 300mT for all particle sizes, although the slopes are steeper for the samples from Middle Creek, MC1 through MC4 suggesting that these samples have lower coercivity than samples from the mine (see Figure 23).

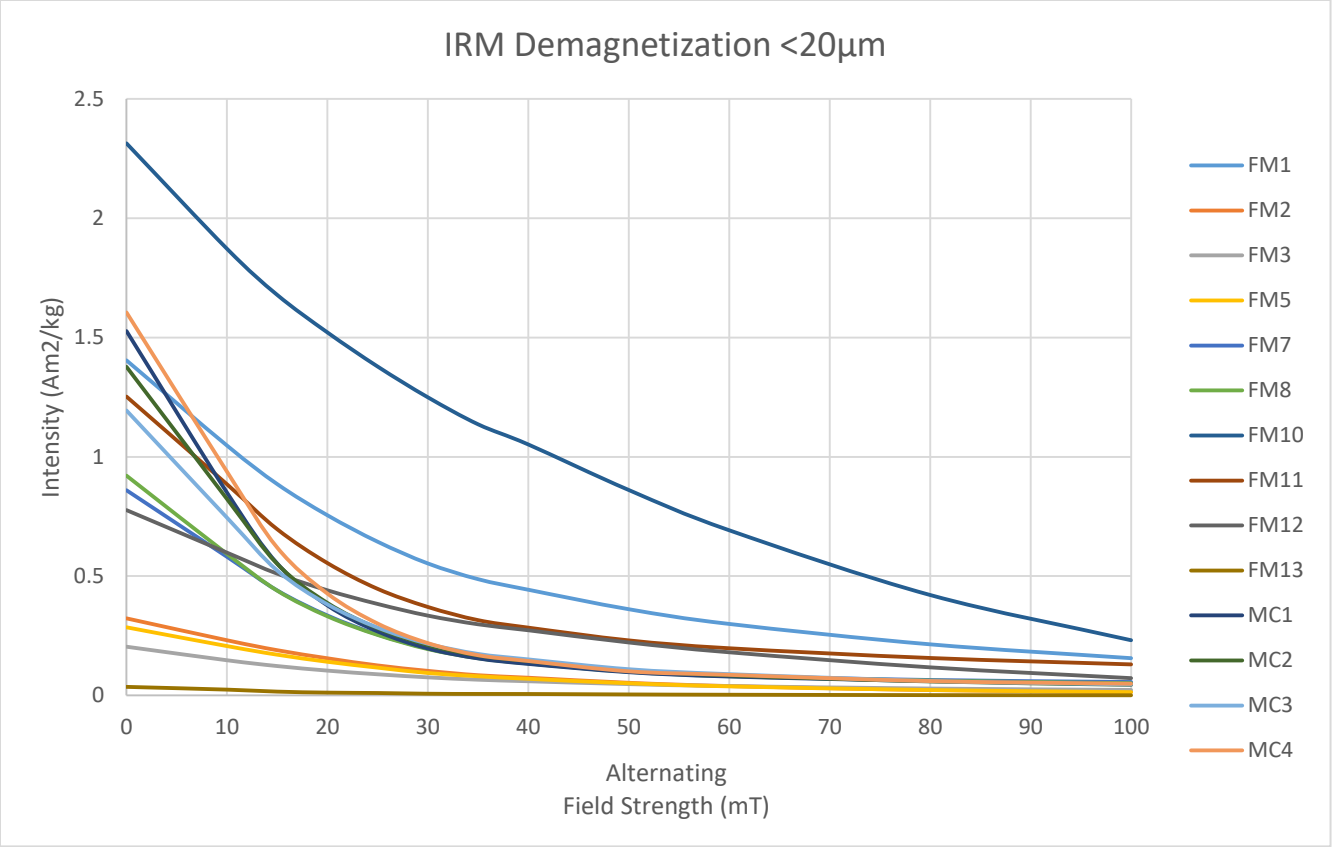

Figure 23- IRM demagnetization curves for all samples under 20µm

The boxplots in Figure 24 indicate significant difference in susceptibility between samples taken from the adit/seeps and samples collected from downstream and the ridge. There is suggestive difference between the samples from the adit/seeps and those from the slope. The ridge and the slope are not significantly different in terms of susceptibility.

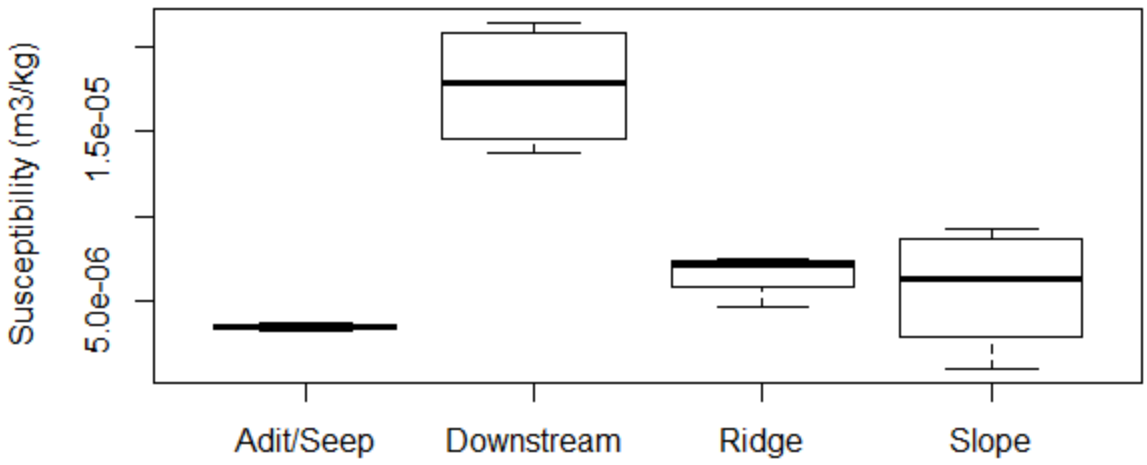

Figure 24- Box and whiskers plot of susceptibility for grouped samples under 20µm

SIRM/X of samples from the adit/seeps and downstream are not significantly different (see Figure 25). Samples from the ridge and slope are also no significantly different but samples from the adit/seeps and downstream are significantly different from those from both the ridge and slope.

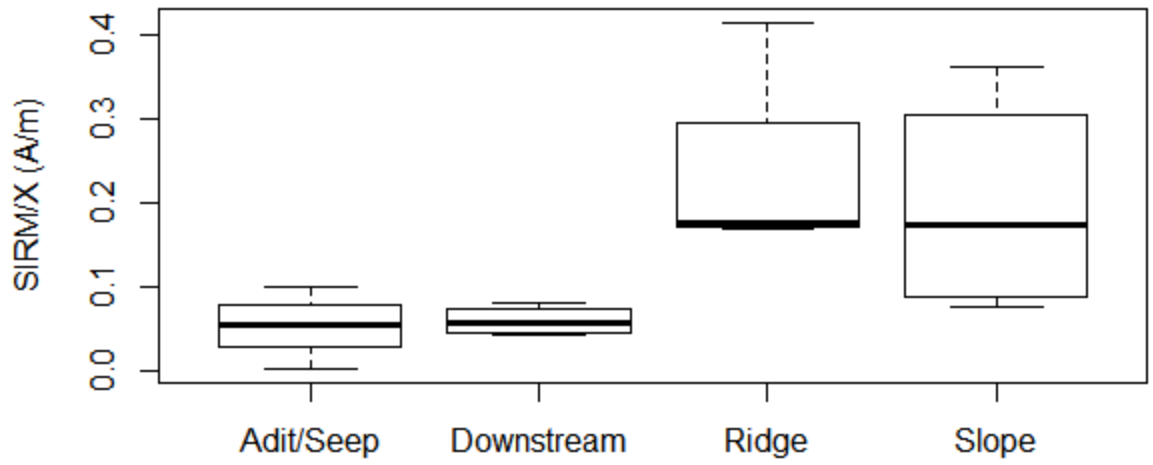

Figure 25- Box and whiskers plot of SIRM/X for grouped samples under 20µm

The concentration of Fe in samples from the adit/seeps is significantly higher than those taken from all other areas (see Figure 26). There is no significant difference between the other 3 groups. For Ti and V there is no significant difference in concentration between any of the groups. Mn is significantly higher in the samples from downstream compared to the samples taken from the mine. At the mine, sampels taken from the slope are significantly lower than those from the ridge but only suggestively different between those from the adit/seeps. The concentration of Zn is significantly lower on the slope than it is in all other places. Samples from the ridge are significantly lower in Zn than those from the adit/seeps and there is evidence that they may be significantly different from those from downstream. There is no evidence to suggest that the concentration of Zn is significantly different between samples from the adit/seeps and those from downstream. Concentrations of Cu are significantly different between the adit/seeps and samples taken from downstream as well as from the slope. There is only suggestive evidence of significant difference between Cu concentration at the adit/seeps compared to the ridge and the ridge compared to the slope. The boxplots indicate that there is no significant difference between the

concentration of Cu in samples from the ridge compared to downstream samples. Ni concentrations are, again, very low or close to zero in the samples from the adit/seeps and ridge. The boxplots show that Ni concentrations taken downstream are significantly higher than those from the slope. Concentrations of As are significantly higher in samples from the adit/seeps compared to all other groups. Those from the ridge and slope show evidence of difference but it is not necessarily significant. Downstream samples have little to no As present.

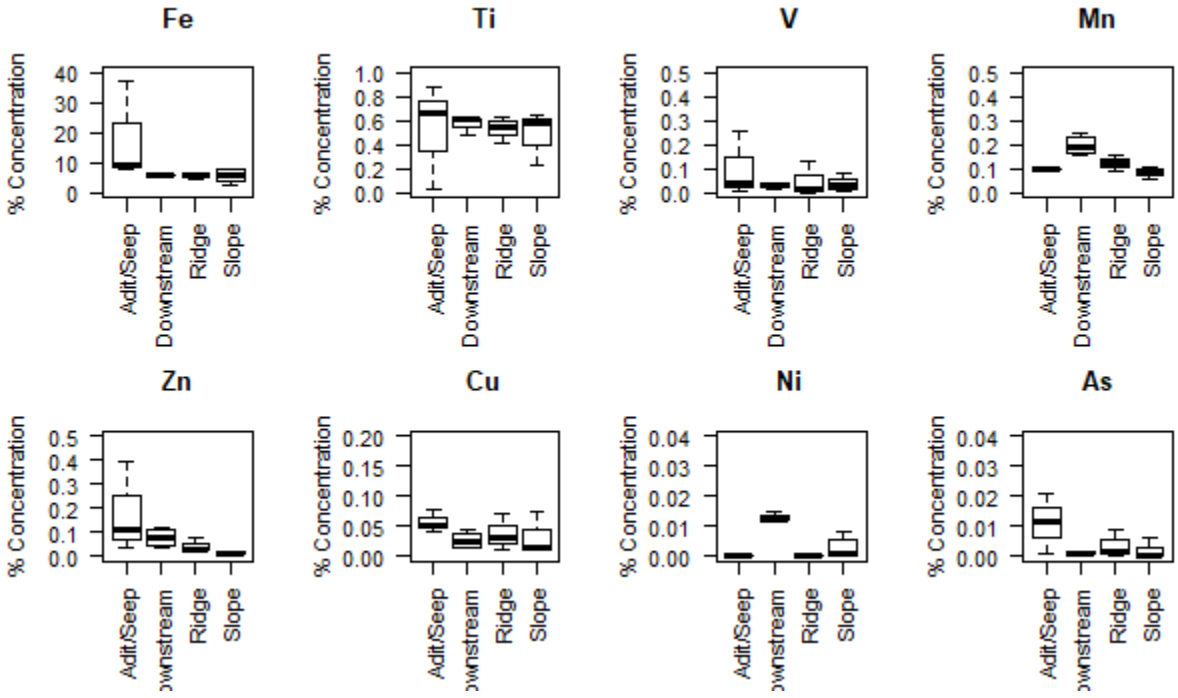

Figure 26- Box and whiskers plots for heavy metal concentrations in grouped samples under 20µm

Regression coefficients between magnetic properties and heavy metal concentrations are presented in Table 5 below. There are strong correlations between Mn and Xlf (0.875) as well as Ni and Xlf (0.888). There are also strong correlations between Fe and Zn (0.92) and Fe and As (0.80) as well as other heavy metals in this fraction.

Table 5- Regression coefficients for correlations between X, SIRM/X and heavy metal concentrations for all samples under 20µm

	Xlf	SIRM/X	Ti	V	Mn	Fe	Ni	Cu	Zn	As
Xlf	1	-0.35548	0.223488	-0.25176	0.875822	-0.22489	0.888181	-0.42088	-0.11159	-0.39326
SIRM/X	-0.35548	1	0.020811	-0.05547	-0.34373	-0.49926	-0.45369	-0.05376	-0.50698	-0.28483
Ti	0.223488	0.020811	1	0.615983	0.23796	-0.60143	0.184698	-0.07319	-0.64594	-0.31743
V	-0.25176	-0.05547	0.615983	1	-0.22095	-0.11698	-0.22872	0.423111	-0.18674	0.407177
Mn	0.875822	-0.34373	0.23796	-0.22095	1	-0.15346	0.789755	-0.29455	-0.03444	-0.29034
Fe	-0.22489	-0.49926	-0.60143	-0.11698	-0.15346	1	-0.21113	0.516231	0.920109	0.803819
Ni	0.888181	-0.45369	0.184698	-0.22872	0.789755	-0.21113	1	-0.35077	-0.04624	-0.39297
Cu	-0.42088	-0.05376	-0.07319	0.423111	-0.29455	0.516231	-0.35077	1	0.560317	0.806332
Zn	-0.11159	-0.50698	-0.64594	-0.18674	-0.03444	0.920109	-0.04624	0.560317	1	0.734182
As	-0.39326	-0.28483	-0.31743	0.407177	-0.29034	0.803819	-0.39297	0.806332	0.734182	1

There are significant correlations between Xlf and Mn and Xlf and Ni (see Table 6). There are also significant correlations between Fe and Ti, Mn and Ni, Ti and Zn, Fe and Zn, Fe and As, Zn and Cu, Cu and As and Zn and As.

Table 6-p-Values for Pearson correlations between X, SIRM/X and heavy metal concentrations for all samples under 20µm

	Xlf	SIRM/X	Ti	V	Mn	Fe	Ni	Cu	Zn	As
Xlf	NA	0.212282	0.442461	0.385233	4.03E-05	0.439535	2.21E-05	0.133976	0.704089	0.164205
SIRM/X	0.212282	NA	0.943705	0.850605	0.228851	0.069133	0.10322	0.85517	0.064275	0.323632
Ti	0.442461	0.943705	NA	0.019	0.412661	0.022896	0.527308	0.803642	0.012578	0.268775
V	0.385233	0.850605	0.019	NA	0.447799	0.690449	0.431559	0.13171	0.522681	0.148463
Mn	4.03E-05	0.228851	0.412661	0.447799	NA	0.600441	0.000779	0.306651	0.906943	0.313939
Fe	0.439535	0.069133	0.022896	0.690449	0.600441	NA	0.468722	0.058782	3.15E-06	0.000531
Ni	2.21E-05	0.10322	0.527308	0.431559	0.000779	0.468722	NA	0.218831	0.875275	0.164547
Cu	0.133976	0.85517	0.803642	0.13171	0.306651	0.058782	0.218831	NA	0.037155	0.000495
Zn	0.704089	0.064275	0.012578	0.522681	0.906943	3.15E-06	0.875275	0.037155	NA	0.002792
As	0.164205	0.323632	0.268775	0.148463	0.313939	0.000531	0.164547	0.000495	0.002792	NA

General Trends

IRM acquisition ratios show that all samples are nearly fully saturated at approximately 300mT. All samples, except FM5 are at least 90% saturated when exposed to a magnetization of 300mT whereas FM5 is only 80% saturated at this field strength. Even at a magnetization of 700mT, this sample is only 93% saturated compared to the other samples which are over 96% saturated. The IRM AF

demagnetization curves indicate that most samples are nearly fully demagnetized by a backfield of 300mT. FM1 and FM10 have higher intensities than the other samples for particle sizes of under 20µm and 20-63µm. For particle sizes over 63µm and the bulk fraction, it is only FM1 that shows much higher intensity.

The ratio of SIRM/X, IRM acquisition and IRM AF demagnetization are significantly different for the samples from Middle Creek compared to the samples from Formosa Mine. In the under 20µm fraction, the samples from Middle Creek have SIRM/X values ranging between 74.9Am-1 to 88.8Am-1. The samples from the mine range between 90.9Am-1 to 323.8Am-1, with FM13 as an extreme outlier with an SIRM/X of 9.7Am-1. In the 20-63m range, the Middle Creek ratios are grouped away from the samples at Formosa Creek but have values ranging from 29.8Am-1 to 78.2Am-1 which is lower than the range for the smaller particle size. FM13 is still an outlier with SIRM/X at 0.9Am-1. Excluding this outlier, the samples from Formosa range from SIRM/X of 53.6Am-1 (FM3) to 243.9Am-1 (FM1). For samples over 63µm, the demarcation between samples from Middle Creek and those from Formosa breaks down. For this particle size there is less variance between the two sets of samples and FM1 and FM9 as the greatest outliers with an SIRM/X of 324.6Am-1 (FM1) and 10.0Am-1 (FM13) compared to the other samples which range between 52.4Am-1 (FM7) and 164.1Am-1 (FM12) (see Figure 4).

Discussion

Potential Factors Influencing Magnetic Properties at Formosa Mine

Reasons for the differences in magnetic properties are complicated to determine without further analysis. They could be caused by variations in lithology, contributions from various land uses in the area or for a number of other reasons. There are several sources of sediment in the samples taken within the creek compared to those taken from the mine. Sloughing and erosion from slopes leading to Middle Creek as well as contributions from sub-basins that feed into it have potential to influence the magnetic signature associated with sediments from the stream.

There are differences between the samples obtained from Middle Creek and those taken from the Formosa Mine. For example, susceptibility of the samples from the stream is much higher than those from the mine, suggesting that there are contributions of harder magnetic material to the sediments in Middle Creek. The saturation isothermal remanence (SIRM) are also much higher for the samples from the creek as compared to those from Formosa Mine. This indicates that these sediments have different mineralogy, specifically in terms of the concentration of ferrimagnetic minerals such as magnetite.

Looking at Figures 17 and 18, the susceptibility of samples from downstream is significantly higher than that of all the other areas sampled. These samples were likely influenced by erosion off the slopes leading into Middle Creek. The most probable explanation for this difference is that magnetic minerals are removed from sediments via redox reactions at the mine. In this case, it is likely that the sediments from Middle Creek are more a reflection of what the natural background magnetic properties would be. Considering that ARD generation leads to the breakdown of iron-bearing minerals, it is plausible that the magnetic properties measured at the mine are a reflection of the processes of oxidation that occur at the Formosa Mine site.

The plots of SIRM/X show that sediments from Middle Creek tend to have finer magnetic grain sizes in the under 20μm fractions than those from Formosa Mine (see Figure 10) with SIRM/X being lowest for the samples from the adit/seeps. This could indicate contributions of sediments from

anthropogenic sources have been altered such that lower coercivity minerals such as magnetite have been removed leaving higher coercivity minerals, such as hematite. Interestingly, these groupings are not found in the 20 to 63m, over 63μm and bulk fractions. In this fraction there are significant differences in SIRM/X between samples from the adit/seeps and those from all other groups. This suggests variation in source of sediments in the finer fractions compared to larger sediment fractions. It is difficult to discern what is controlling SIRM/X in the finer fractions (under20 and 20 to 63m) for samples from downstream and the ridge. SIRM/X is significantly higher for downstream samples compared to the adit/seeps for particles under 20m whereas for particles between 20 and 63m the ridge has significantly higher SIRM/X compared to downstream samples. For the larger particle size fractions, the pattern of higher SIRM/X is consistently higher for samples from the slope and ridge at Formosa compared to both downstream and adit/seeps samples. This suggests that there are processes acting on the magnetic properties of the finer particle sizes that may not affect larger particles.

Isothermal remanent magnetization reaches saturation around 300mT in all samples from both the mine and the stream. This indicates that magnetite is likely the dominant magnetic mineral in these samples. There are distinct differences in the rate of acquisition of the three samples taken near adits and seeps compared to the other samples from the mine. Looking at Figure 22 (IRM AQ <20), these three samples show more gradual acquisition than the other samples from the site. The samples from Middle Creek have steep acquisition curves and reach saturation at lower field strengths than those taken from the mine. FM10 is an outlier, different from all other samples. This sample was taken near a well that was close to the road running through the site.

Samples taken from the Formosa Mine show some interesting results. The lowest susceptibility (FM3) was measured in a sample that was taken from a vegetated area downslope from the encapsulation mound. The highest susceptibility was from the roadside cut bank where sediments were exposed but mixed with soils rather than just waste rock. Interestingly, samples that were taken from areas adjacent to seeps and/or adits had lower IRM intensities than samples obtained elsewhere. Both of these observations

support the theory that sediments affected by mining processes have been depleted of magnetic minerals relative to natural background sediments/soils.

SIRM/X is an indicator of magnetic mineralogy and or magnetic grain size. The sample that stands out from the rest most significantly is FM13, which was taken adjacent to the adit where the diversion system is located. Acid rock drainage flows from the adit by the diversion system, which does not function as intended. It is possible that ARD is influencing the mineralogy of sediments near this adit. Water flowing from this adit has been measured to have pH values as low as 2. This represents a highly acidic environment, which could potentially alter mineralogy.

Significant differences in heavy metal concentrations are found between different areas for some of the metals detected by XRF. Elevated levels of Fe at the adit and seeps are likely related to the presence of water and precipitation of Fe from solution by oxidation. Indeed, there are iron precipitates visible at the adit and in drainage paths leading away from seeps.

Processes Affecting Heavy Metal Concentrations

Acid Rock Drainage and pH

Exposure of waste materials to the environment in terms of precipitation and oxygen determines their potential to create ARD and MIW. The bedrock material is a massive sulfide ore body consisting primarily of pyrite (FeS2), chalcopyrite (CuFeS2) and sphalerite (ZnS) (CDM, 2009). A series of oxidation reactions creates ferric iron which is highly reactive in oxidized environments, leading to acid generation by the following reactions (CDM, 2012). The first reaction describes oxidation of pyrite in the presence of water to form ferrous iron, sulfate and hydrogen.

$$FeS_2 + 3.5O_2 + H_2O \rightarrow Fe^{2+} + 2SO_4^{2-} + 2H^+$$

Further oxidation leads to formation of ferric iron (second equation) which has potential to react with pyrite to generate further acidity by its behavior as an oxidant in solution, as described in the third equation of this sequence (CDM, 2012).

$$Fe^{2+} + 0.25O_2 + H^+ \rightarrow Fe^{3+} + 0.5H_2O$$

$$FeS_2 + 14Fe^{3+} + 8H_2O \rightarrow 15Fe^{2+} + 16H^+ + 2SO_4^{2-}$$

The underground network is highly connected and there are several seeps through which ARD is transported to the creeks (CDM, 2012). In addition, the aquifer beneath the encapsulation mound and other perched aquifers on site contribute as sources of ARD. Surface materials consist of low grade waste rock and other mine materials which also have potential to generate ARD (CDM, 2012). All toll, it is estimated that anywhere from 4 million to 12 million cubic gallons of ARD are generated at the site each year (CDM, 2009; CDM, 2012).

There are several activities that create waste materials with potential to cause ARD. These include mineral extraction processes such as blasting, tunneling and excavation of ore; mineral beneficiation processes such as separation floatation and smelting; and mine materials management which involves dealing with waste materials and mine reclamation, ultimately determining the distribution of these materials on the landscape (CDM, 2009).

The underground water network consists of three zones; the permanently unsaturated zone, seasonally saturated zone and permanently saturated zone (CDM, 2012). ARD and MIW are generated year round in the permanently unsaturated zone with pulses of higher acidity resulting from heavier rain events that flush out the seasonally saturated zone (CDM, 2012). The permanently saturated zone generates the least amount of ARD (CDM, 2012).

Inputs of water from adjoining streams could influence pH in Middle Creek and other streams affected ARD from Formosa. Contributions of water from streams that are not affected by ARD could increase the pH of stream water by dilution and/or contributions of carbonates that neutralize acidic water (Hammarstrom et al., 2003). As pH levels rise, some heavy metals may precipitate from solution, some may adsorb to soil surfaces and others may form complexes with other heavy metals or minerals (Gammons et al., 2005; Hamarstrom et al., 2003)

Adsorption of Metals from Acid Rock Drainage and Mining Influenced Water

Heavy metals are generally attracted to iron-bearing minerals, however this is largely dependent on pH. Lin (1997) concludes that adsorption of heavy metals to iron-bearing minerals occurs primarily in the clay fraction of sediments and that heavy metals concentrate where iron precipitates form. Exposure to oxygen raises acidity and increases mobilization of heavy metals (Lin, 1997). In another study by Quispe et al. (2013), the authors find that there is seasonal retention of the metals Cd, Co, As, Ni, Cu and Mn by sulfate salts which are flushed out in the wet season. Such may be the case at Formosa Mine, which, like the study area in the Quispe et al. (2013) report, has a seasonally saturated zone where water accumulates through the drier months and is flushed out in the wet season.

There is evidence to suggest that heavy metals associate with iron-bearing minerals at the Formosa Mine for the finer particle size fractions (under 20m and 20 to 63m). Significant correlations between Fe and Cu, Zn and As are found for the 20 to 63m fraction while in the under 20m fraction, there is significant correlation between Fe and Zn and Fe and As, but only strong evidence of a significant correlation between Fe and Cu. Both Cu and As are more abundant in the adit/seeps samples compared to samples from other areas, as is Fe. Although the complexation of these metals with iron-bearing minerals has not been assessed, it is likely that these metals associate with each other in this particular environment.

Limitations of Study

There are several sources of error apparent in this study. They have to do with timing of sampling, the spatial pattern of sampling, variations in volume of sediment sampled, presence/absence of organic materials in samples, and a number of other factors.

Variations in the volume of sediment subsampled introduces error in the susceptibility measurements. The containers for measurements in the susceptibility meter, and magnetometer are $8cm^3$.

If the containers are not filled, cotton balls are used to fill in the empty space. The more sediment in a sample, the less error is introduced to the overall measurement.

There is serious bias in terms of the spatial distribution of samples. Samples taken from Middle Creek are spread apart at distances spanning several kilometers. Despite the distance between them, the samples from the creek show similar results in terms of having lower coercivity than the samples from the mine. Samples from the mine are much more concentrated with the total area sampled being smaller than the distance between points on Middle Creek. Although there are obvious differences in magnetic properties between each group of samples, the comparison lies on two very different scales. As such, there is little that can be said in terms of relating these differences to local factors, without having more information.

Spatial autocorrelation is an issue when comparing the samples taken from each site, however, there is greater variation in magnetic properties observed from the mine, where the samples are closer together compared to those from Middle Creek. The first law of geography states that conditions at distances that are closer together are more similar than those that are farther apart. The scale to which this law is true has not been determined for this site. A more random sampling design is needed to draw conclusions regarding the spatial distribution of magnetic properties both at the site and throughout the basin. Better coverage of conditions associated with specific features would allow for more robust assessment of whether or not spatial autocorrelation is a concern at this site. It is also assumed that there is contribution of sediments from the mine to sediments downstream. Given the stark differences in magnetic properties and concentrations of heavy metals between the samples taken from the mine and those downstream, it is unlikely that sediments from the mine have a significant impact on the areas sampled in Middle Creek. Sampling farther upstream, closer to the mine and on the scale of sampling done at the mine might paint a different picture. The gradient expected, if it even exists, cannot be detected with the sampling done for this study.

In the case of this study, it would have been useful to obtain several samples taken randomly from areas surrounding known features, such as the adit diversion, encapsulation mound and seeps around the

mine. This way, differences in properties could be postulated with respect to processes that affect these features. Taking several samples would allow for more robust statistical analysis of variation in magnetic properties, thereby increasing confidence in the results and subsequent explanations for those differences.

Overall, limitations of this study are primarily due to timing and spatial distribution of sampling. The design could be improved by taking samples from both areas within the same time period(s) and by randomizing the spatial distribution of samples, or stratifying and nesting samples based on a-priori knowledge of site features and accessibility to various areas.

Further Exploration

Meaningful spatial analysis of patterns would require a sampling design that captures spatial heterogeneity. A sampling design where samples were taken over a gradient in elevation leading down to the stream would capture variations in magnetic properties and/or heavy metals from the mine into the stream. Samples could be taken at set distances along the stream to get a clearer picture of changes as a function of distance from the mine. Taking cores at various elevations would capture details on infiltration and downslope movement of metals as well as provide records of variation in magnetic properties with depth. Collecting samples from streams that feed into Middle Creek would allow for assessment of the contribution of sediments from other land use in the area, including other mines, logging sites and agriculture.

Collecting core samples as opposed to bulk surface samples would yield information about how magnetic properties and heavy metal concentrations vary with depth. This information would be useful in assessing and establishing background characteristics for more meaningful comparison between past and current conditions. In order to truly establish background characteristics, cores should be taken to a depth that reaches and samples the underlying bedrock. This was not done in this study.

Better information on heavy metal concentrations would increase confidence in the correlations between them and magnetic parameters of interest. This could be achieved by using different

methodology such as atomic adsorption spectrometry or induced coupled plasma mass spectrometry which have capabilities of detecting a wider range of heavy metals at concentrations that are much lower than those detectable by x-ray fluorescence.

Conclusions

In conclusion there are significant differences in magnetic properties and some heavy metal concentrations of sediments collected from different areas of the mine and downstream. Differences can be related to source of the samples both at the mine (adit/seeps, ridge and slope) and downstream in Middle Creek. The most notable difference is the higher susceptibility of sediments obtained from Middle Creek, compared to those from the mine. This finding is in contrast to the hypothesis that higher susceptibility would be associated with mining activities.

It was postulated that magnetic properties that are highly correlated with concentrations of metals could potentially be used as proxy for determining hot spots of heavy metal contamination. There are some correlations between heavy metals that suggest they are attracted to iron-bearing minerals (Fe with As, Zn and Cu), however these metals are not correlated with magnetic properties, according to the analysis performed in this study. The only correlations between heavy metals and magnetic properties occur in the under 20m fraction between X and Mn and X and Ni. Without further exploration, reasons for these correlations cannot be deduced. It is not likely that magnetic properties can be related to heavy metal concentrations at this site.

Despite the conclusion that magnetic properties do not provide a useful proxy for mapping heavy metal hotspots at the mine, there are clear differences in magnetic properties between the mine and samples taken downstream. There is evidence to suggest that magnetic properties alone may provide insight into sources of sediments to Middle Creek. Further exploration and expansion of sampling efforts to capture local heterogeneity of magnetic properties related to different land use could provide an interesting glimpse into the factors that affect magnetic properties in this watershed.

References

Ariztegui D, Chondrogianni C, Lami A, Guilizzoni P, Lafargue E. **2001**. Lacustrine organic matter and the Holocene paleoenvironmental record of Lake Albano (central Italy). *Journal of Paleolimnology*. **26** : 283–292.

Bureau of Land Management. 2015. Abandoned Mine Lands Portal. Online http://www.abandonedmines.gov/. Accessed November 15, 2016.

Bloemendal, J., King, J.W., Hall, F.R. and S.J. Doh. **1992**. Rock magnetism of late Neogene and Pleistocence deep-sea sediments: Relation to sediment source, diagenetic processes and sediment lithology. *Journal of Geophysical Research*. **97**: 4361-4375.

CDM Federal Programs Corporation. **2009**. Final Data Summary Report, Formosa Superfund Site, Douglas County, OR. United States Environmental Protection Agency.

CDM Federal Programs Corporation. **2012**. Final OU1 Remedial Investigation Report, Formosa Superfund Site, Douglas County, OR. Volume 1-Text. United States Environmental Protection Agency.

CDM Federal Programs Corporation. **2013**. Final OU1 Feasibility Report Formosa Mine Superfund Site, Douglas County, OR. United States Protection Agency.

Chaparro MAE, Bidegain JC, Sinito AM, Jurado SS, Gogorza CSG. **2004.** Magnetic studies applied to different environments (soils and stream sediments) from a relatively polluted area in Buenos Aires Province, Argentina. *Environmental Geology*. **45** : 654–664. DOI: 10.1007/s00254-003-0915-x

Chaparro MAE, Chaparro MAE, Marinelli C, Sinito AM. **2008a**. Multivariate techniques as alternative statistical tools applied to magnetic proxies for pollution: a case study from Argentina and Antarctica. *Environmental Geology*. **54** : 365–371. DOI: 10.1007/s00254-007-0823-6

Chaparro MAE, Sinito AM, Ramasamy V, Marinelli C, Chaparro MAE, Mullainathan S, Murugesan S. **2008b**. Magnetic measurements and pollutants of sediments from Cauvery and Palaru River, India. *Environmental Geology*. **56** : 425–437. DOI: 10.1007/s00254-007-1180-1

Charlesworth SM, Lees JA. **2001**. The application of some mineral magnetic measurements and heavy metal analysis for characterising fine sediments in an urban catchment, Coventry, UK. *Journal of Applied Geophysics*. **48** : 113–125.

Clements, B.M., Javier, J., Sah, J.P. and M.S. Ross. **2010**. The effects of wildfires on magnetic properties of soils in the Everglades. *Earth Surface Processes and Landforms*. **34**: 460-466.

Dearing, J. **1994**. Environmental magnetic susceptibility. Bartington Instruments, Witney, Oxon, England, 104 pp.

Gammons, C.H., Nimick, D.A., Parker, S.R., Cleasby, T.E., and R.B. McCleskey. **2005**. Diel behavior of iron and other heavy metals in a mountain stream with acidic to neutral pH: Fisher Creek, Montana, USA. *Geochimica et Cosmochimica Acta*. **69**: 2505-2516.

Gautam P, Blaha U, Appel E. **2005**. Integration of magnetism and heavy metal chemistry of soils to quantify the environmental pollution in Kathmandu, Nepal. *Island Arc*. **14** : 424–435.

Hammarstrom, J.M., Seel, R.R., Meier, A.L., and J.C. Jackson. **2003**. Weathering of sulfidic shale and copper mine waste: secondary minerals and metal cycling in Great Smoky Mountains National Park, Tennessee, and North Carolina, USA. *Environmental Geology*. **43**: 35-57.

Heller F, Strzyszcz Z, Magiera T. **1998**. Magnetic record of industrial pollution in forest soils of Upper Silesia, Poland. *Journal of Geophysical Research: Solid Earth*. **103** : 17767–17774.

Hoffmann V, Knab M, Appel E. **1999**. Magnetic susceptibility mapping of roadside pollution. *Journal of Geochemical Exploration*. **66** : 313–326.

Hu X-F, Su Y, Ye R, Li X-Q, Zhang G-L. **2007**. Magnetic properties of the urban soils in Shanghai and their environmental implications. *Catena*. **70** : 428–436. DOI: 10.1016/j.catena.2006.11.010

Kapička A, Petrovskỳ E, Ustjak S, Macháčková K. **1999.** Proxy mapping of fly-ash pollution of soils around a coal-burning power plant: a case study in the Czech Republic. *Journal of Geochemical Exploration*. **66**: 291–297.

Lecoanet H, Leveque F, Ambrosi J-P. **2003**. Combination of magnetic parameters: an efficient way to discriminate soil-contamination sources (south France). *Environmental Pollution*. **122** : 229–234.

Lin, Z. **1997**. Mobilization and retention of heavy metals in mill-tailings from Garpenberg sulfide mines, Sweden. *The Science of the Total Environment*. **198**: 13-31.

Lisé-Pronovost A, St-Onge G, Brachfeld S, Barletta F, Darby D. **2009**. Paleomagnetic constraints on the Holocene stratigraphy of the Arctic Alaskan margin. *Global and Planetary Change*. **68** : 85–99. DOI: 10.1016/j.gloplacha.2009.03.015

Liu Q, Roberts AP, Larrasoaña JC, Banerjee SK, Guyodo Y, Tauxe L, Oldfield F. **2012**. Environmental magnetism: Principles and applications. *Reviews of Geophysics*. **50** DOI: 10.1029/2012RG000393 [online] Available from: http://doi.wiley.com/10.1029/2012RG000393 (Accessed 10 September 2014)

Lu SG, Bai SQ. **2006**. Study on the correlation of magnetic properties and heavy metals content in urban soils of Hangzhou City, China. *Journal of Applied Geophysics*. **60** : 1–12. DOI: 10.1016/j.jappgeo.2005.11.002

Maher BA. **2007**. Environmental magnetism and climate change. *Contemporary Physics*. **48** : 247–274. DOI: 10.1080/00107510801889726

Maher BA, Thompson R (eds). **1999**. Quaternary Climates, Environments and Magnetism . Cambridge University Press: Cambridge [online] Available from: http://ebooks.cambridge.org/ref/id/CBO9780511535635 (Accessed 10 October 2016)

Morton-Bermea O, Hernandez E, Martinez-Pichardo E, Soler-Arechalde AM, Santa-Cruz RL, Gonzalez-Hernandez G, Beramendi-Orosco L, Urrutia-Fucugauchi J. **2009**. Mexico City topsoils: Heavy metals vs. magnetic susceptibility. *Geoderma.* **151** : 121–125. DOI: 10.1016/j.geoderma.2009.03.019

Oldfield F, Hunt A, Jones MDH, Chester R, Dearing JA, Olsson L, Prospero JM. **1985**. Magnetic differentiation of atmospheric dusts. *Nature*. **317**

Petrovský E, Ellwood BB. **1999**. Magnetic monitoring of air- land- and water-pollution. In Quaternary Climates, Environments and Magnetism , Maher BA and Thompson R (eds). Cambridge University Press: Cambridge; 279–322. [online] Available from: http://ebooks.cambridge.org/ref/id/CBO9780511535635A015 (Accessed 10 October 2016)

Quispe, D., Perez-Lopez, R., Acero, P., Ayora, C. and J.M. Nieto. **2013**. The role of mineralogy on element mobility in two sulfide mine tailings from the Iberian Pyrite Belt (SW Spain). *Chemical Geology*. **345**: 119-129.

Robertson DJ, Taylor KG, Hoon SR. **2003.** Geochemical and mineral magnetic characterisation of urban sediment particulates, Manchester, UK. *Applied Geochemistry*. **18** : 269–282.

Sapkota B, Cioppa MT. **2012**. Using magnetic and chemical measurements to detect atmospherically-derived metal pollution in artificial soils and metal uptake in plants. *Environmental Pollution*. **170** : 131–144. DOI: 10.1016/j.envpol.2012.06.010

Shu J, Dearing JA, Morse AP, Yu L, Yuan N. **2001**. Determining the sources of atmospheric particles in Shanghai, China, from magnetic and geochemical properties. *Atmospheric Environment*. **35** : 2615–2625.

St-Onge G, Chapron E, Guyard H, Rochon A, Lajeunesse P, Locat J, Scott D, Stoner JS, Hillaire-Marcel C. **2008**. High-resolution physical and magnetic properties of rapidly deposited layers associated with landslides, earthquakes and floods. Locat, J.(Éd.) Geohazards. Presses de l'Université Laval, Québec, Canada [online] Available from: http://www.geohazards.ggl.ulaval.ca/technologies/st_onge.pdf (Accessed 10 September 2014)

Thompson R, Oldfield F. **1986**. Environmental Magnetism . Springer Netherlands: Dordrecht [online] Available from: http://link.springer.com/10.1007/978-94-011-8036-8 (Accessed 10 October 2016)

Verosub KL, Roberts AP. **1995**. Environmental magnetism: Past, present, and future. Journal of *Geophysical Research: Solid Earth*. **100** : 2175–2192. DOI: 10.1029/94JB02713

Wang B, Xia D, Yu Y, Jia J, Xu S. **2014**. Detection and differentiation of pollution in urban surface soils using magnetic properties in arid and semi-arid regions of northwestern China. *Environmental Pollution*. **184** : 335–346. DOI: 10.1016/j.envpol.2013.08.024

Zhang C, Appel E, Qiao Q. **2013**. Heavy metal pollution in farmland irrigated with river water near a steel plant--magnetic and geochemical signature. *Geophysical Journal International*. **192** : 963–974. DOI: 10.1093/gji/ggs079

Zhang C, Qiao Q, Appel E, Huang B. **2012**. Discriminating sources of anthropogenic heavy metals in urban street dusts using magnetic and chemical methods. *Journal of Geochemical Exploration*. **119**–**120** : 60–75. DOI: 10.1016/j.gexplo.2012.06.014

Zhang C, Qiao Q, Piper JDA, Huang B. **2011**. Assessment of heavy metal pollution from a Fe-smelting plant in urban river sediments using environmental magnetic and geochemical methods. *Environmental Pollution*. **159** : 3057–3070. DOI: 10.1016/j.envpol.2011.04.006